Executive Summary

S.1 INTRODUCTION

The Interagency Monitoring of Protected Visual Environments (IMPROVE) program is a cooperative measurement effort between the U. S. Environmental Protection Agency (EPA), federal land management agencies, and state agencies. The network is designed to

1. establish current visibility and aerosol conditions in 156 mandatory Class I areas (CIAs);
2. identify chemical species and emission sources responsible for existing anthropogenic visibility impairment;
3. document long-term trends for assessing progress towards the national visibility goal;
4. provide regional haze monitoring representing all visibility-protected federal CIAs where practical.

Although the program is focused on visibility objectives, the data acquired and the methodologies developed by the IMPROVE network have been broadly used to address air quality management related to human health, climate change, ecosystem degradation, and material damage.

This IMPROVE report is the sixth in a series that describes the monitoring methods and changes to instrumentation over time, as well as reports on measured aerosol concentrations and aerosol-derived visibility estimates. This report does not include data summaries of the network's direct atmospheric optical monitoring using nephelometers. The IMPROVE[1] and FED[2] web sites include descriptions of the aerosol, optical, and scene monitoring activities and provide access to the aerosol and optical data.

Air quality measurements in the IMPROVE network began in 1988. Due to resource and funding limitations in the early network, measurements in all 156 mandatory CIAs were not possible. Instead, 36 sites were selected to represent aerosol concentrations and visibility over the United States. The first IMPROVE report was published in 1993 and described data that were collected at the initial 36 sites from March 1988 through February 1991 (Sisler et al., 1993). Beginning with the initial report, and in the reports that followed, spatial patterns and seasonal trends in speciated aerosol concentrations and reconstructed light extinction coefficients (b_{ext}) were presented. In addition, the first report focused on aerosol measurement quality, aerosol acidity, and transmissometer measurements. In 1996 the second IMPROVE report was published and described data from March 1992 through February 1995 from 43 sites in the network (Sisler et al., 1996). In addition to spatial and seasonal trends, the second report included an exploration of aerosol light extinction efficiencies and long-term trends in fine mass and sulfur, using stacked filter unit measurements. In 2000, the third IMPROVE report was produced that included descriptions of data from 49 sites during the period from March 1996 through February 1999 (Malm et al., 2000). This report also included a discussion of the contributions of aerosol species to periods of high and low mass concentrations. Temporal (long-

[1] The IMPROVE website (http://vista.cira.colostate.edu/Improve/).
[2] The Federal Environmental Database (FED) website (http://views.cira.colostate.edu/fed/).

term and diurnal) trends in visibility and aerosol concentration were also reported. The fourth report was published in 2006 and covered data from 2000 through 2004 (Debell et al., 2006). The number of sites increased to 159 due to the expansion of the network to meet the goals of the Regional Haze Rule (RHR). In addition to data from the IMPROVE sites, data from 84 sites from the EPA's Speciated Trends Network (STN) were included to expand the spatial and seasonal aerosol and b_{ext} trends to include urban areas and to investigate the differences in urban and rural aerosol concentrations. The 2006 report also included an initial investigation into the comparability of IMPROVE and STN (now Chemical Speciation Network, CSN) data. Focus was also placed on IMPROVE quality assurance procedures. In 2011 the fifth IMPROVE report was published that covered data from 2005–2008 (Hand et al., 2011), and the network consisted of 212 sites (170 current and 42 discontinued sites). Analyses of data from EPA's CSN were also included. Spatial and seasonal trends in aerosol mass and b_{ext} were reported for major aerosol species, including sea salt. The additional analyses in the fifth report included an examination of urban and rural aerosol differences ("urban excess") and their spatial patterns using IMPROVE and CSN data. A deeper exploration of the seasonality in speciated aerosol mass concentrations and b_{ext} was also presented. With the long temporal record of IMPROVE data, "long-term" (1989–2008) and "short-term" (2000–2008) trends in speciated aerosol concentrations for seasonal and statistical parameters were explored. Descriptions of regional haze metrics, including comparisons of visibility between the RHR baseline period (2000–2004) and period 1 (2005–2009) were presented.

The sixth IMPROVE report covers analyses of data from 2016–2019. At the timing of this report, the IMPROVE network consisted of 229 sites (159 current and 70 discontinued sites). Data from the CSN were also included. Analyses of the spatial variability in aerosol mass and b_{ext} as well as regional and seasonal variability are included for major aerosol species. Long-term (1990-2019) and short-term (2000-2019) trends in speciated aerosol concentrations for annual, seasonal, and percentiles are reported. Several supporting Appendices are also included. The following summary provides highlights of the material contained in the sixth (2023) IMPROVE report; the reader is encouraged to refer to the full report for additional details.

S.2 AEROSOL DATA

The version II IMPROVE sampler, deployed in 2000, consists of four independent modules (A, B, C, and D) that collect 24-hour samples every third day from midnight to midnight at local time and the data are reported at local conditions. Each module incorporates a separate inlet, filter pack, and pump assembly. Modules A, B, and C are equipped with a 2.5 µm cyclone that allows for sampling of particles with aerodynamic diameters less than 2.5 µm, while module D is fitted with a PM_{10} inlet to collect particles with aerodynamic diameters less than 10 µm. Each module contains a filter substrate specific to a particular chemical analysis. Module A is equipped with a PTFE (polytetrafluoroethylene) Teflon® filter (referred to as "Teflon") that is analyzed for $PM_{2.5}$ gravimetric fine mass, elemental concentration, and filter light absorption. Module B is fitted with a Nylasorb (nylon) filter and analyzed for the anions sulfate, nitrate, nitrite, and chloride using ion chromatography. Module C utilizes a quartz fiber filter that are analyzed by thermal optical analysis (TOA) for organic and elemental carbon (Chow et al., 1993). Finally, module D utilizes a Teflon filter that is analyzed for PM_{10} gravimetric mass.

Details regarding aerosol sampling and analyses are in Chapter 1. IMPROVE data are available for download from the Federal Environmental Database (FED, http://views.cira.colostate.edu/fed/). Current and discontinued IMPROVE sites are listed by region in Table 1.1 in Chapter 1. A map of IMPROVE sites (grouped by region) is shown in Figure S.2.1.

CSN data were also used extensively in this report. CSN sites are operated by state, local, and tribal agencies, primarily in urban/suburban settings (Solomon et al., 2014). All CSN samplers utilize a $PM_{2.5}$ inlet and three channels containing Teflon, nylon, and quartz filters. Like the IMPROVE network, CSN samplers operate on a 24-hour schedule from midnight to midnight every third or sixth day. Elemental compositions are analyzed from the Teflon filter, ions from the nylon filter, and carbon from the quartz filter. CSN stopped analyzing $PM_{2.5}$ gravimetric mass beginning in 2014, and collocated data from EPA Federal Reference Method (FRM) sites were used. IMPROVE and CSN sampling and analysis methods for each species are provided in Chapter 1 and discussions of aerosol species mass calculations are in Chapter 2. A map of CSN sites is provided in Figure S.2.2. A subset of these sites was used in this report, based on completeness criteria outlined in Chapter 2.

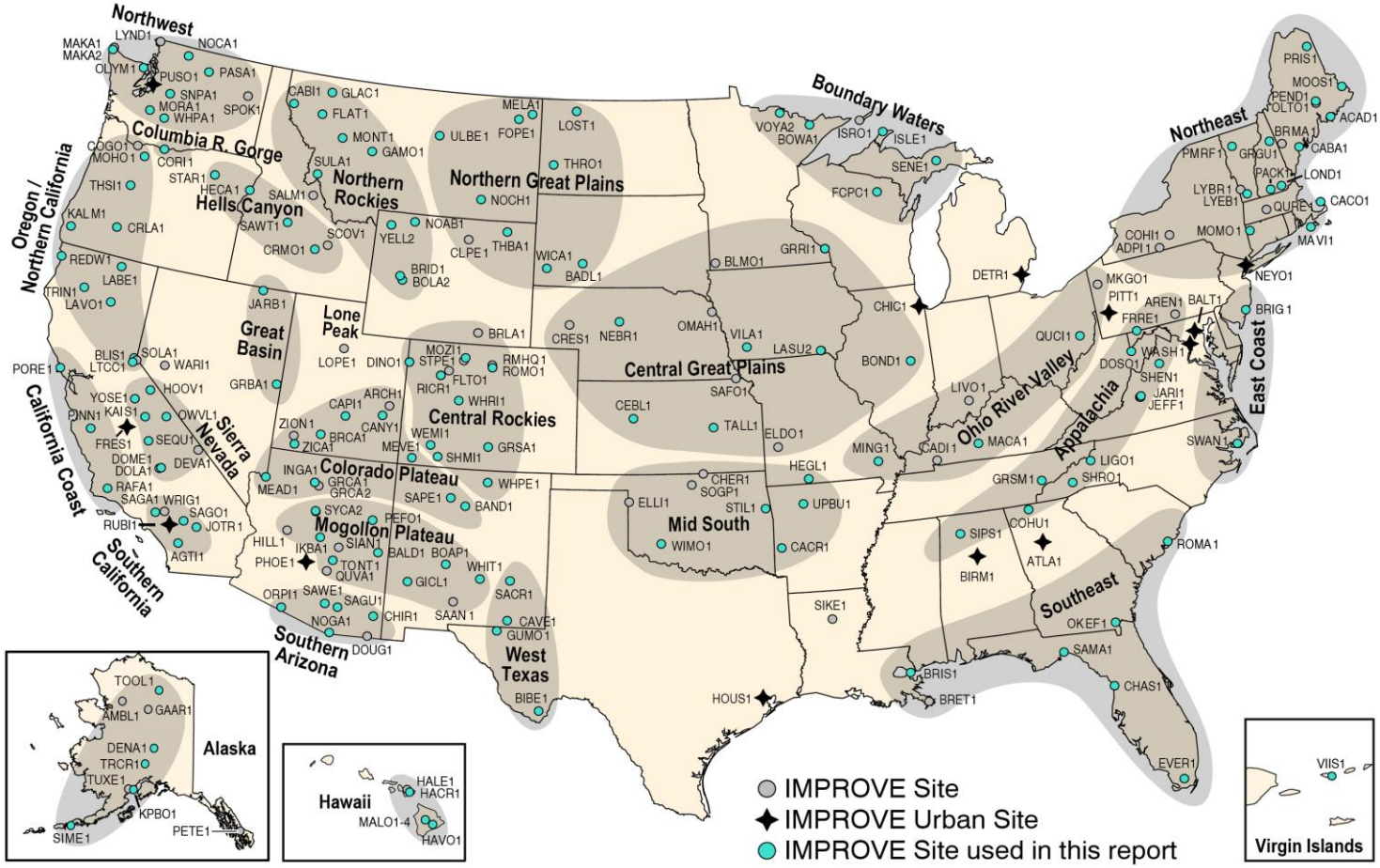

Figure S.2.1. Locations of IMPROVE sites for all discontinued and current sites. IMPROVE regions are indicated by shading and bold text. Urban IMPROVE sites are identified by stars. Blue circles indicate sites with data used in the analyses in this report.

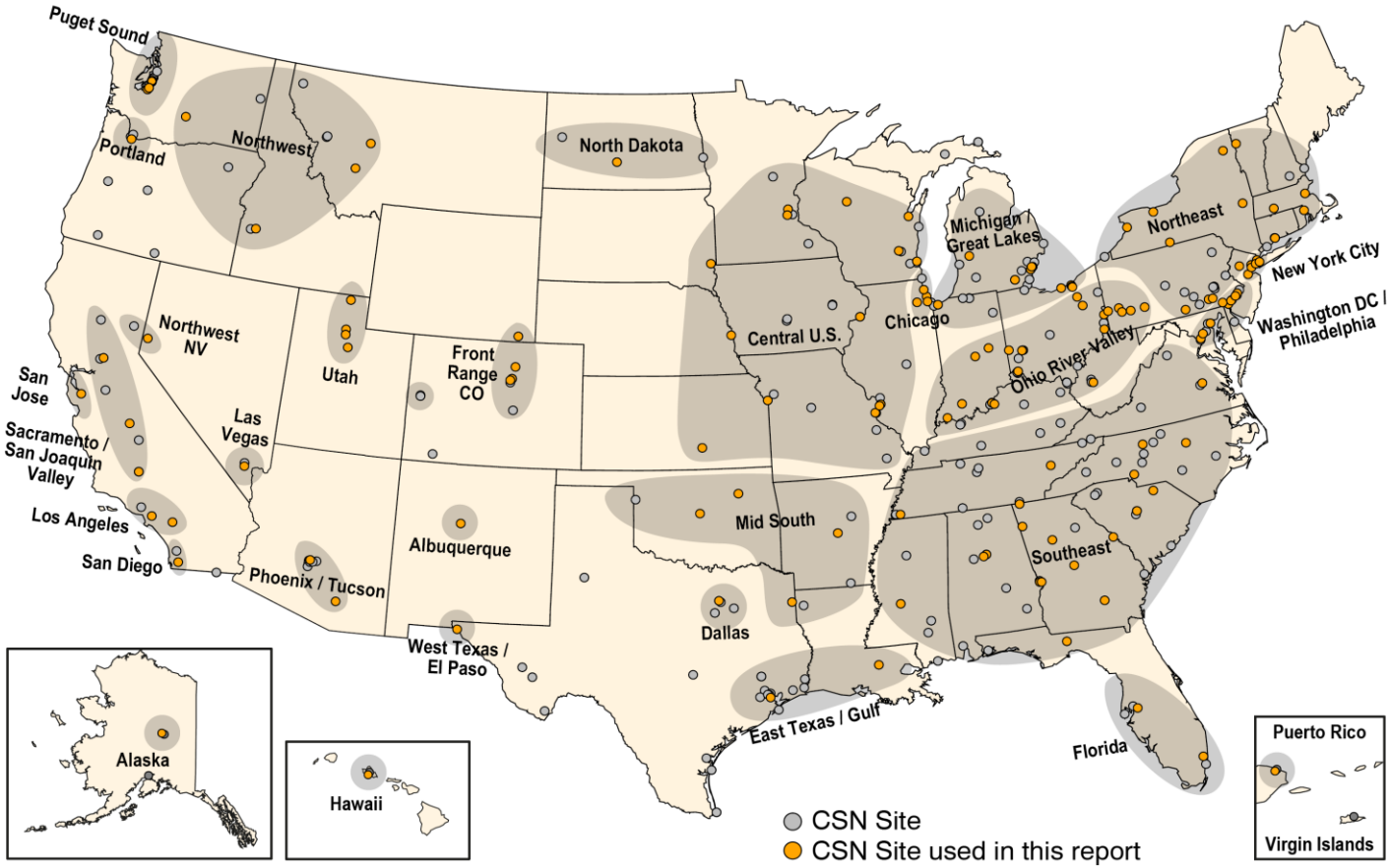

Figure S.2.2. Current and discontinued Chemical Speciation Network (CSN) sites (grey and orange) operated by the Environmental Protection Agency. Regions are shown as shaded areas and bold text. Sites included in the analyses in this report are shown as orange circles.

The IMPROVE and CSN networks operate collocated samplers in several urban/suburban sites. Collocated sites with data that met the completeness criteria outlined in Chapter 2 were compared to identify relative biases between IMPROVE and CSN speciated aerosol concentrations. Monthly mean data from Birmingham, Alabama; Fresno, California; Phoenix, Arizona; and Puget Sound, Washington, for 2016–2019 were compared for ammonium sulfate (AS), ammonium nitrate (AN), organic carbon (OC), elemental carbon (EC), fine dust (FD), sea salt (SS), $PM_{2.5}$ gravimetric fine mass (FM), and reconstructed fine mass (RCFM, the sum of $PM_{2.5}$ species). Descriptions of species mass concentrations calculations are listed in Table 2.1 in Chapter 2. Table S.2 provides comparison statistics. Errors were less than 20% for most species, with the exception of FD (21%) and SS (85%). IMPROVE SS concentrations were computed using chloride ion concentrations ($1.8 \times Cl^-$), whereas CSN SS concentrations were computed using chlorine concentrations ($1.8 \times Cl$) from (X-ray fluorescence) XRF analysis. CSN began reporting chloride concentrations in February 2017. Errors for EC were 19%, in part due to changes in TOA for CSN. Biases were typically within ±15%, except for a -20% bias in FD (IMPROVE higher), -81% bias in SS (IMPROVE higher), and 21% bias in EC (CSN higher). Higher biases and errors associated with coarse-mode species may be due in part to differences in the sharpness of the cut points between IMPROVE and CSN samplers, with sharper CSN cut points resulting in lower concentrations, because less of the tail of the coarse-mode species is collected on the $PM_{2.5}$ filter. Additional comparisons between IMPROVE and CSN data are described in Gorham et al. (2021).

Table S.2. Comparisons between monthly mean data at collocated IMPROVE and CSN sites from 2016 through 2019. Species include organic carbon (OC), elemental carbon (LAC), ammonium sulfate (AS), ammonium nitrate (AN), fine dust (FD), sea salt (SS), $PM_{2.5}$ gravimetric fine mass (FM), and $PM_{2.5}$ reconstructed fine mass (RCFM, sum PM2.5 species). Positive biases correspond to higher CSN concentrations.

Statistic	OC	EC	AS[3]	AN[4]	FD	SS[5]	FM	RCFM
Average IMPROVE ($\mu g\ m^{-3}$)	2.36	0.69	1.21	1.44	1.21	0.24	8.58	9.04
Average CSN ($\mu g\ m^{-3}$)	2.59	0.84	1.15	1.40	0.90	0.05	9.42	9.01
Bias[1] (%)	11	21	-6	-6	-20	-81	9	-1
Error[2] (%)	11	19	6	8	21	85	10	4
r	0.99	0.97	0.99	1.00	0.96	0.71	0.97	0.99
IMP/CSN	0.91	0.82	1.06	1.03	1.34	4.75	0.91	1.00

[1] $\text{Error} = \text{median}\left(\left|\frac{\overline{X}_i - \overline{Y}_i}{\overline{Y}_i}\right|\right)$

[2] $\text{Bias} = \frac{1}{N}\sum_i^N \frac{\overline{X}_i - \overline{Y}_i}{\overline{Y}_i}$; $\overline{X}_i$ and $\overline{Y}_i$ are the daily data for CSN and IMPROVE concentrations, respectively. The number of data points is given by N.

[3] AS = 1.375×[sulfate ion]

[4] AN = 1.29×[nitrate ion]

[5] Sea salt = 1.8×[chloride ion] for IMPROVE and 1.8×[chlorine] for CSN.

S.3 SPATIAL PATTERNS IN RURAL AND URBAN SPECIATED ANNUAL MEAN AEROSOL CONCENTRATIONS

Data from 153 IMPROVE and 136 CSN sites that met completeness criteria were combined to explore the spatial variability in the 2016–2019 annual mean concentrations in

major aerosol species. Shown here is a summary of the results in Chapter 2, including spatial variability for AS, AN, particulate organic matter (POM), calculated from OC and a monthly (IMPROVE) or seasonal (CSN) varying organic carbon to organic mass ratio (OM/OC) (POM = (OM/OC) × OC), EC, SS, FD, FM, and coarse mass (CM = PM_{10} - $PM_{2.5}$). Urban $PM_{2.5}$, PM_{10}, and CM were obtained from the EPA FRM network sites. Maps of interpolated annual mean mass concentrations were created for each species for IMPROVE data alone, and for combined IMPROVE and CSN data. Isopleth maps created using a Kriging algorithm (Isaaks and Mohan Srivastava, 1989) should be viewed and interpreted with caution, as these maps are intended only to help visualize the data and identify large spatial patterns. Maps and discussions of fractional contributions from each $PM_{2.5}$ species to RCFM can be found in Chapter 2.

S.3.1 Ammonium Sulfate

The spatial distribution of AS with the rural IMPROVE sites alone (Figure S.3.1a) was very similar to the pattern of the rural and urban (CSN) sites combined (Figure S.3.1b), suggesting that regional impacts of AS concentrations similarly influenced both urban and rural sites. Notice the difference in site density between the IMPROVE and CSN networks in Figure S.3.1.b, with many more CSN sites in the eastern United States; these sites provide additional detail to the spatial patterns of AS in that section of the country. The combination of high sulfur dioxide (SO_2) emissions and high relative humidity produced the highest concentrations (2-3 μg m^{-3}) of AS in the eastern United States that centered on the Ohio River valley and Mid-south areas. AS concentrations decreased sharply towards the western United States. In fact, concentrations in the western United States were typically less than 1 μg m^{-3}, with the lowest concentrations at sites in the Northwest, Montana, and Idaho. Lower concentrations in the West reflected lower SO_2 emissions that lead to secondary particulate AS.

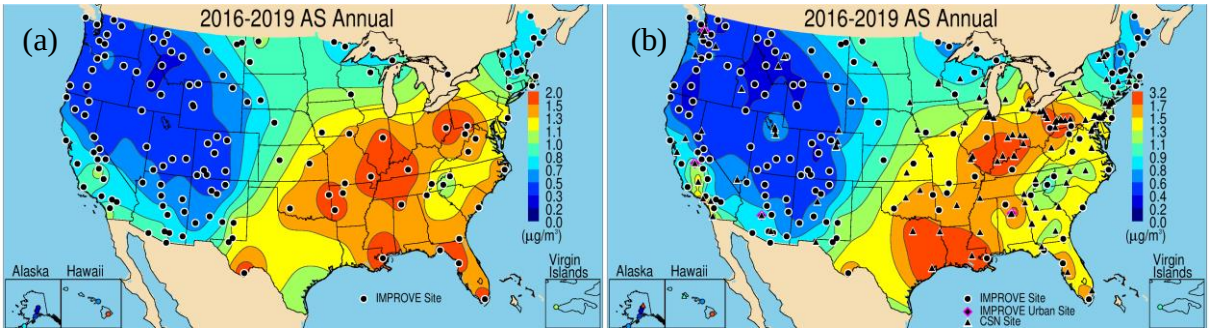

Figure S.3.1. 2016–2019 $PM_{2.5}$ ammonium sulfate (AS) annual mean mass concentrations (μg m^{-3}) for (a) IMPROVE and (b) IMPROVE and CSN.

S.3.2 Ammonium Nitrate

Higher sources of precursors to AN in agricultural regions in the Midwest resulted in the highest AN concentrations (~2 μg m^{-3}) for rural sites in the United States (Figure S.3.2a). Generally, urban concentrations of AN were considerably higher than rural concentrations (Figure S.3.2b). Central and southern California were also associated with higher AN concentrations, as were sites in northern North Dakota, with concentrations near 1.0 μg m^{-3}. High concentrations in North Dakota may be associated with oil and gas energy development (Prenni

et al., 2016; Evanoski-Cole et al., 2017; Gebhart et al., 2018). Concentrations were much lower outside of the central United States, especially in the Intermountain West and Northwest, with concentrations less than 0.5 μg m^{-3}. Similarly low annual mean concentrations were observed at sites in the Southeast and Northeast. The inclusion of CSN sites provided more spatial resolution to the rural AN spatial pattern and showed the impact of urban AN concentrations on surrounding areas. High annual mean AN concentrations were associated with urban sites near Lake Michigan, and other hot spots near Denver, Colorado and Salt Lake City, Utah.

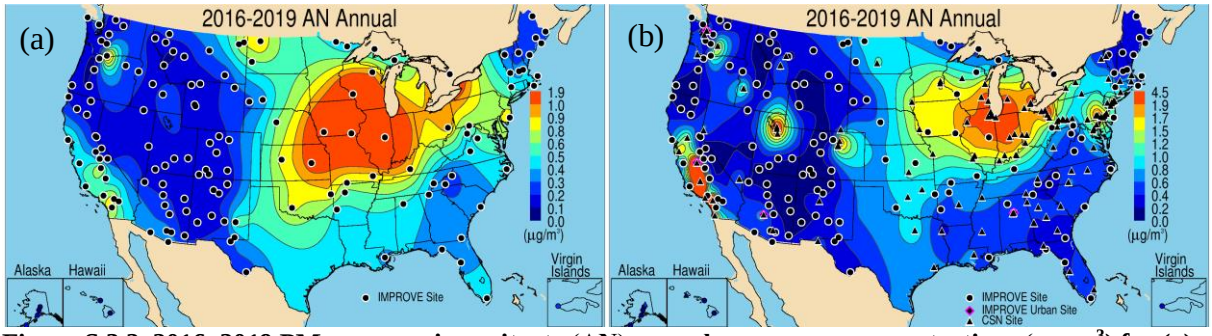

Figure S.3.2. 2016–2019 $PM_{2.5}$ ammonium nitrate (AN) annual mean mass concentrations (μg m^{-3}) for (a) IMPROVE and (b) IMPROVE and CSN.

S.3.3 Particulate Organic Matter

The highest 2016–2019 annual mean rural IMPROVE POM concentrations occurred at sites in southern Florida, the northwestern United States, and central and northern California due to the influence of biomass burning (Figure S.3.3a). Elevated levels of POM (~3.0 μg m^{-3}) also occurred at sites in the Southeast, as well as portions of the Northwest and California. The 2016–2019 period was associated with high fire activity, especially 2017 and 2018 in the Northwest and 2016 in the Southeast. The combined urban and rural POM concentrations demonstrated the influence of urban POM sources, with higher concentrations at sites in the Southeast and along the Central Valley of California (Figure S.3.3b). Sites in Alabama, Georgia, South Carolina, and North Carolina had POM concentrations greater than 4.0 μg m^{-3}. Similar maximum annual mean rural and urban POM concentrations demonstrated the influence of biomass burning on rural POM concentrations.

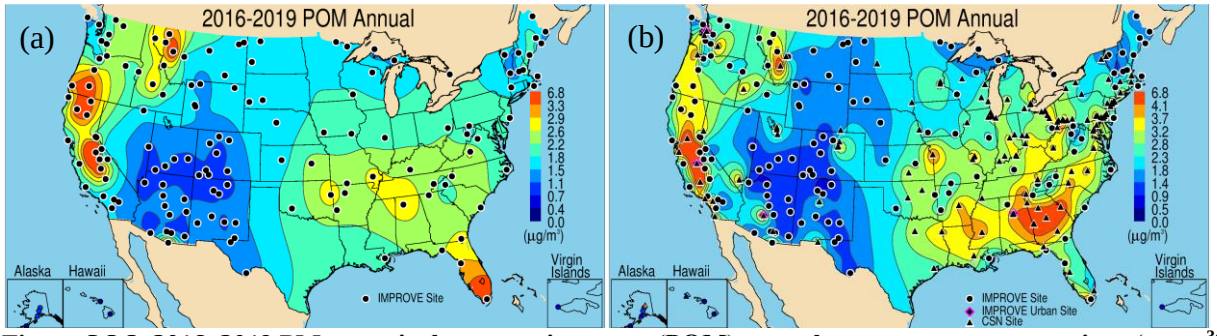

Figure S.3.3. 2016–2019 $PM_{2.5}$ particulate organic matter (POM) annual mean mass concentrations (μg m^{-3}) for (a) IMPROVE and (b) IMPROVE and CSN.

S.3.4 Elemental Carbon

The IMPROVE rural 2016–2019 annual mean EC concentrations were higher at sites in California and the Northwest (~0.25 μg m^{-3}), and at sites in the central and eastern United States (>0.25 μg m^{-3}; see Figure S.3.4a). Urban CSN EC concentrations were generally higher than at IMPROVE sites (Figure S.3.4b). Regionally, urban EC concentrations were highest at sites in the East; however, most impacts of EC were local in extent. Several hot spots occurred in major urban areas, for example, at sites in Colorado, Montana, and Nevada, and several sites in the Central Valley of California. The urban hot spots were indicative of local urban EC emissions (e.g., mobile sources or local residential wood burning) rather than regional sources like biomass combustion from controlled or wild fires. The steep spatial gradient surrounding the hot spots of EC in Figure S.3.4b indicated that the spatial extent of the impact was small and concentrations diluted quickly before they had regional impacts.

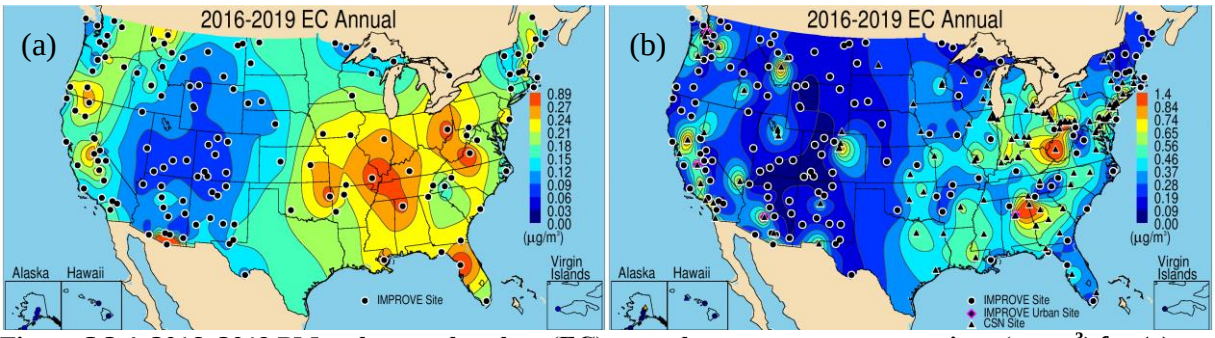

Figure S.3.4. 2016–2019 $PM_{2.5}$ elemental carbon (EC) annual mean mass concentrations (μg m^{-3}) for (a) IMPROVE and (b) IMPROVE and CSN.

S.3.5 Fine Dust

The patterns observed in the 2016–2019 annual mean rural IMPROVE FD concentrations were reflective of dominant seasons of elevated FD concentrations, namely the Southwest during spring and the Southeast during summer (Hand et al., 2017). Concentrations at sites around Arizona ranged from 1.3 to 3.1 μg m^{-3}. Sites around the Colorado Plateau as well as sites in southern New Mexico and western Texas had annual mean concentrations near 1 μg m^{-3} (see Figure S.3.5a). Unlike other species with spatial gradients along the east/west orientation, gradients in FD concentrations extended north/south. The concentrations at northern sites tended to be lower (~0.5 μg m^{-3}). Although the CSN FD concentrations were biased low relative to IMPROVE concentrations, the spatial patterns in combined urban and rural FD generally agreed, with higher concentrations at sites in the Southwest (Figure S.3.5b). There were several urban hot spots with elevated FD concentrations, such as sites in Colorado, Nevada, Missouri, and Texas. Sites in the Central Valley of California had higher FD concentrations relative to surrounding areas.

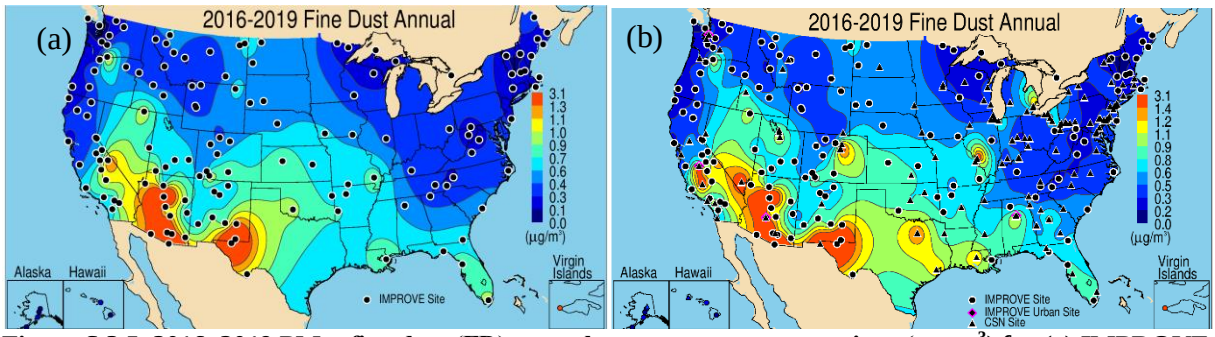

Figure S.3.5. 2016–2019 $PM_{2.5}$ fine dust (FD) annual mean mass concentrations (µg m^{-3}) for (a) IMPROVE and (b) IMPROVE and CSN.

S.3.6 Sea Salt

The IMPROVE sites with the highest 2016–2019 annual mean SS concentrations were along coastal regions (~ 2 µg m^{-3}, Figure S.3.6a). Outside of coastal regions, SS concentrations were low (<0.10 µg m^{-3}). The spatial patterns were generally similar when aggregating IMPROVE and CSN data (Figure S.3.6b), even with the bias between IMPROVE and CSN SS concentrations.

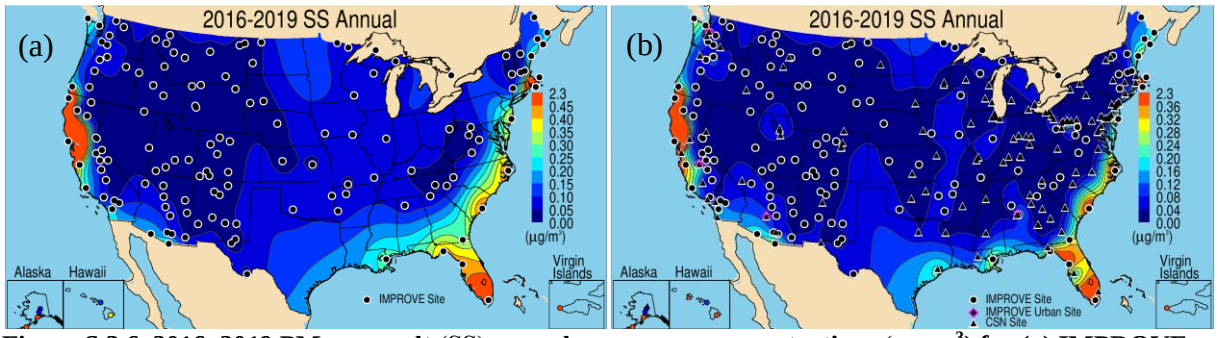

Figure S.3.6. 2016–2019 $PM_{2.5}$ sea salt (SS) annual mean mass concentrations (µg m^{-3}) for (a) IMPROVE and (b) IMPROVE and CSN.

S.3.7 $PM_{2.5}$ Gravimetric Mass

The spatial pattern of 2016–2019 annual mean IMPROVE FM concentrations reflected the combined patterns of annual mean concentrations of AS, AN, and POM (see Figure S.3.7a). Sites in the central and eastern United States had relatively high annual mean FM concentrations (~5–6 µg m^{-3}). In addition, sites in California's Central Valley had higher concentrations. The lowest FM concentrations occurred in the Intermountain West. The urban FM concentrations were somewhat higher than the IMPROVE concentrations, especially at sites in the central and eastern United States (Figure S.3.7b). High annual mean urban FM was also observed at sites in the Central Valley of California, where the highest urban annual mean FM (~13 µg m^{-3}) occurred. Several hot spots of annual mean FM occurred at urban sites across the West, such as sites in Colorado, Texas, Utah, Montana, and Washington.

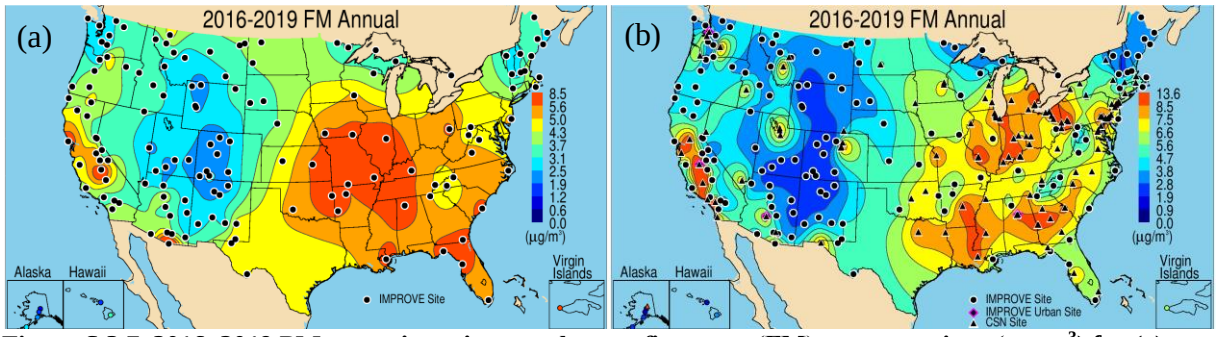

Figure S.3.7. 2016–2019 $PM_{2.5}$ gravimetric annual mean fine mass (FM) concentrations (µg m^{-3}) for (a) IMPROVE and (b) IMPROVE and CSN.

S.3.8 Coarse Mass

The spatial patterns of CM in the Southwest were similar to those of FD and suggest similar sources (Hand et al., 2017). Higher concentrations also occurred at sites in the California's Central Valley (Figure S.3.8a). At sites in the central United States, higher concentrations most likely corresponded to agricultural activity and fugitive dust sources (Hand et al., 2019a; Lambert et al., 2020). Lower annual mean CM concentrations occurred at sites across the Intermountain West, the Northwest, and along the eastern United States into the Northeast. The overall spatial patterns in urban annual mean CM concentrations (Figure S.3.8b) were similar to those at rural sites, with higher values at sites in the central United States and along the U.S.–Mexico border and California's Central Valley.

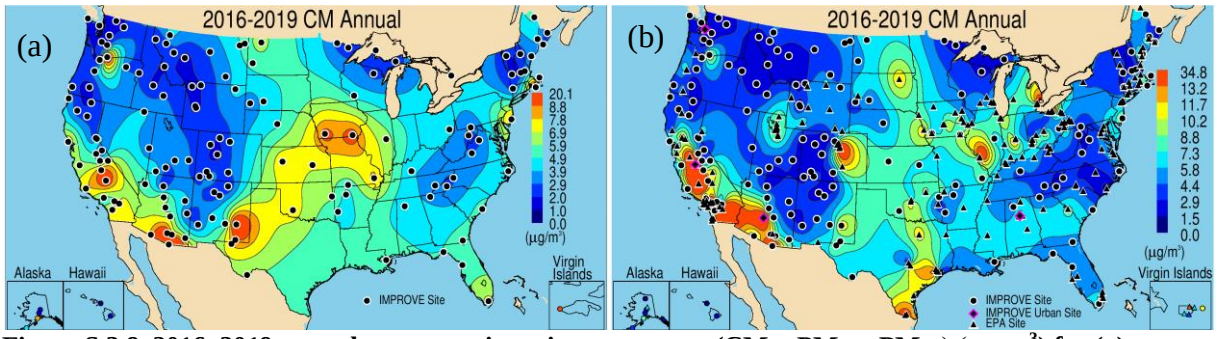

Figure S.3.8. 2016–2019 annual mean gravimetric coarse mass (CM = PM_{10} - $PM_{2.5}$) (µg m^{-3}) for (a) IMPROVE and (b) IMPROVE and EPA.

S.3.9 Discussion

The spatial variability of FM depends on sources, sinks, and transport of speciated aerosols. A strong spatial gradient in FM was observed, with higher concentrations at sites in the eastern United States. FM decreased rapidly moving westward, with concentrations that were half of those at sites in the East, especially for sites in the Intermountain West. Higher concentrations occurred at sites in California and sites in Oregon and Washington. The spatial patterns did not change significantly with the addition of urban sites, although urban concentrations were higher, including several hot spots at sites in the West, and at sites in the Central Valley of California. The lowest concentrations of annual mean FM occurred at sites in the Intermountain West and Southwest and at sites in the Northeast.

The spatial patterns of FM reflected the combined patterns of AS, AN, and POM. AS concentrations were highest in the eastern United States, where SO_2 emissions were highest, and AS contributed approximately 30% to FM in those regions. Rural annual man AN concentrations were highest at sites in the central United States and contributed 20%-30% to FM at sites in that region. Additional urban sources influenced urban FM sites in the Central Valley of California, as well as other urban hot spots in the West.

Rural POM concentrations were highest at sites in the northwestern United States, where biomass smoke impacts influenced concentrations, and at sites in the eastern United States, due to biogenic emissions and biomass smoke. The lowest annual mean POM concentrations occurred at sites in the Intermountain West and Southwest. The general spatial patterns of urban and rural POM concentration were similar to rural-only patterns, although higher urban concentrations occurred at sites in Southeast and Central Valley. Contributions of POM to RCFM were significant at sites in the western United States, around 70% or greater, and this contribution was similar for CSN sites. At sites in the eastern United States, contributions at CSN sites was around 60% or greater, while for rural sites it was around 50%. Annual mean EC concentrations followed similar patterns to those of POM concentrations at rural sites, with higher concentrations at sites both in the eastern and northwestern United States. Urban EC concentrations were considerably higher than at rural sites, indicating the importance of localized urban sources. Contributions of EC to RCFM at urban sites were roughly double relative to at rural sites (~10% compared to ~5%, respectively).

The spatial pattern of FD reflected its source areas, with high concentrations at both rural and urban sites in the Southwest, where local and regional sources affect FD concentrations. Sites in the Central Valley also had high FD concentrations, especially for urban sites. Higher annual mean FD at sites in the Southeast reflected the influence of North African dust transport to that area, both for rural and urban sites. FD contributions to RCFM at sites in the Southwest were over 50% for many sites in the region. The spatial variability in annual mean CM was similar to FD, especially for sites in the Southwest, suggesting similar sources. However, higher annual mean CM at sites in the central United States, relative to FD patterns, suggested additional sources of coarse-mode aerosol or larger size distributions of FD relative to the Southwest. Urban sites with high CM concentrations occurred in the Central Valley and southern Arizona. CM contributed significantly to PM_{10}, especially at sites in the western United States, where annual mean contributions were over 60%. For sites in the eastern United States, the contribution of CM to PM_{10} was ~30-40%. Similar contributions occurred for sites in the Northwest.

SS concentrations, while likely underestimated, also followed suspected marine sources, with higher values along coastal areas for both IMPROVE and CSN sites. SS contributions could be significant (>10%) at some sites, especially in Alaska and Hawaii, and along the coasts.

S.4 SEASONAL DISTRIBUTIONS IN AEROSOL MASS CONCENTRATIONS

The seasonality of speciated aerosol mass concentrations can be significant depending on species and region and is a function of the source emissions, meteorological parameters, formation processes, and local and long-range transport. Examining aerosol concentrations on a

regional basis, rather than a site-specific basis, can lead to insights regarding air quality issues on regional scales.

IMPROVE and CSN data from 2016 through 2019 were regionally and monthly averaged (see Chapter 3) and plotted as stacked bar charts on maps of three areas of the United States (i.e., East, Northwest, and Southwest). The monthly mean concentrations of $PM_{2.5}$ species included AS, AN, POM, EC, FD, and SS. Stacked bar charts provide a detailed view of the changes in monthly mean aerosol concentrations during the year at different regions in the United States. Highlights in seasonality of mass concentrations for IMPROVE and CSN concentrations are included here; additional detail, including regional mass fractions, are provided in Chapter 3.

S.4.1 Ammonium Sulfate

In most of the regions in the eastern United States, regional mean AS concentrations rarely exceeded 2 $\mu g\ m^{-3}$ year round (Figure S.4.1). In addition, the monthly variability of AS was flat, with a small increase in summer months in some regions (e.g., MidSouth and East Coast). Monthly mean concentrations in regions in the northwestern United States were lower than in the eastern United States (typically <1 $\mu g\ m^{-3}$) and had little seasonal variability (see Figure S.4.2). The highest mean AS concentrations in regions in the northwestern United States occurred in the Northern Great Plains and Columbia River Gorge regions, where concentrations approached 1 $\mu g\ m^{-3}$. AS concentrations in the regions of the southwestern United States (Figure S.4.3) were generally <2 $\mu g\ m^{-3}$ and demonstrated more of a summer peak (e.g., Southern California, Southern Arizona, and West Texas regions). Low monthly mean concentrations (<1 $\mu g\ m^{-3}$) were observed in the Great Basin, Colorado Plateau, and Central Rockies regions. In the Hawaii region, monthly mean AS concentrations were >1 $\mu g\ m^{-3}$ for most months of the year.

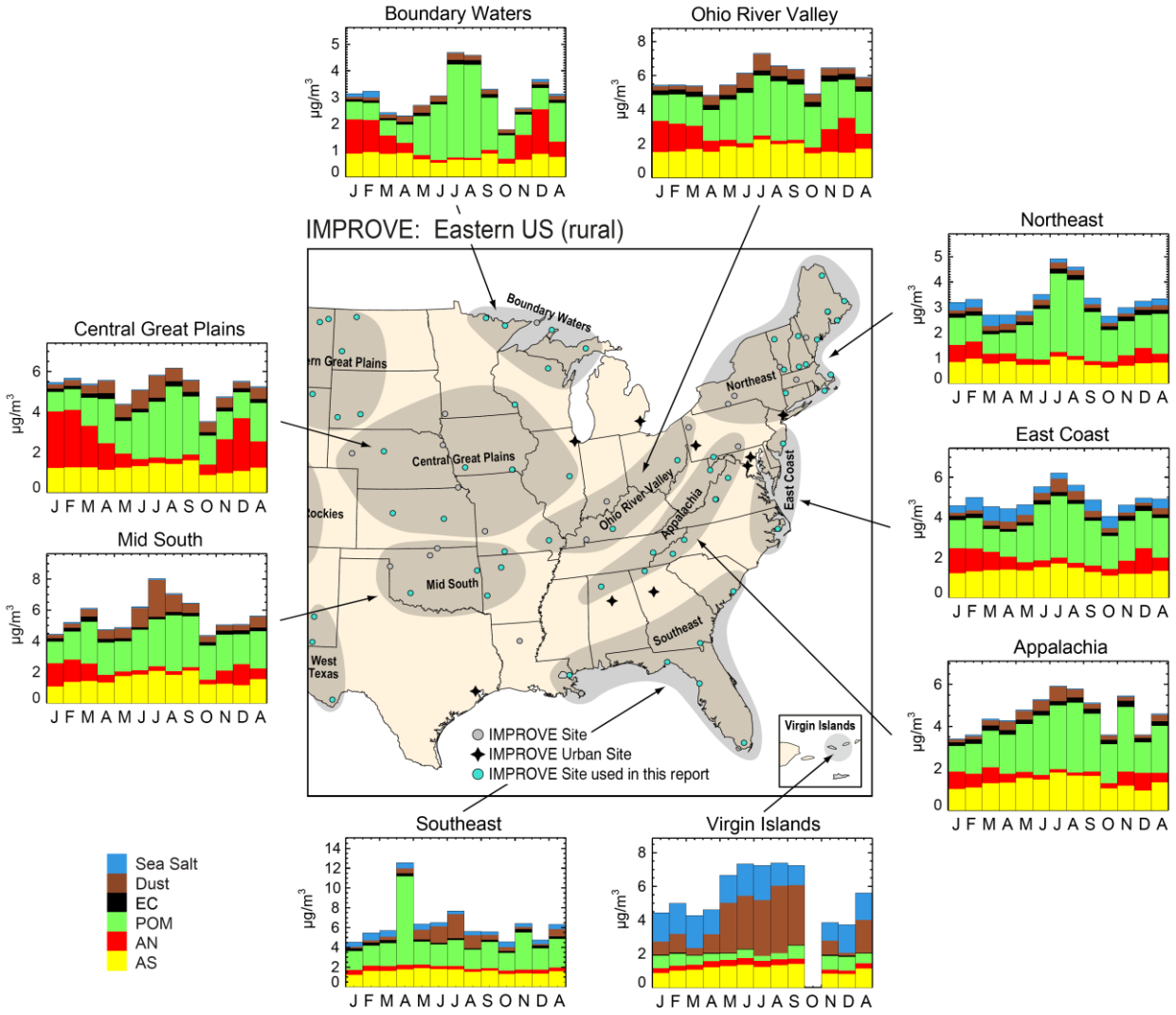

Figure S.4.1. IMPROVE 2016–2019 regional monthly mean $PM_{2.5}$ mass concentrations (µg m^{-3}) for the eastern United States. Letters on the x-axis correspond to month and "A" corresponds to annual mean. Shaded areas in the map correspond to regions that include the sites used in the analysis, shown as blue dots.

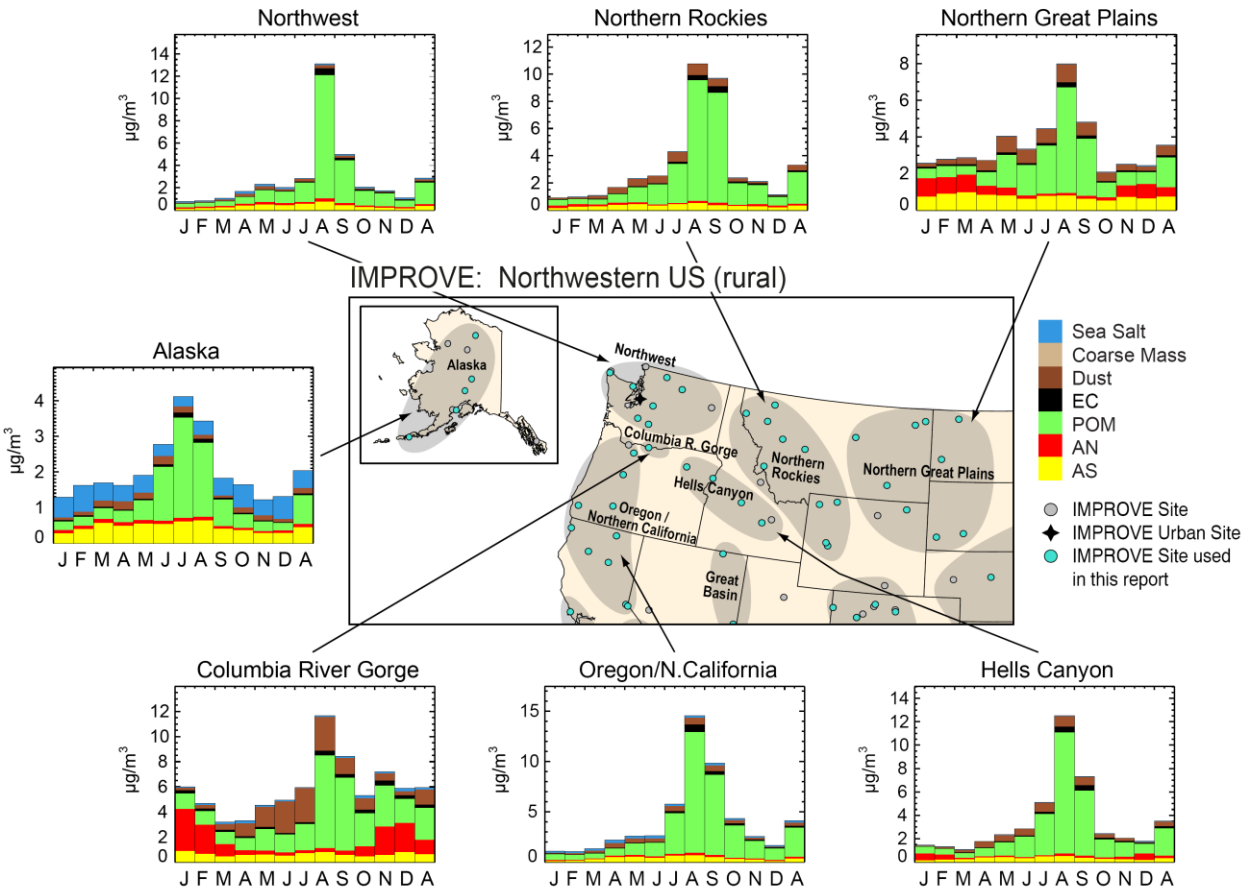

Figure S.4.2. IMPROVE 2016–2019 regional monthly mean $PM_{2.5}$ mass concentrations (µg m^{-3}) for the northwestern United States. Letters on the x-axis correspond to month and "A" corresponds to annual mean. Shaded areas in the map correspond to regions that include the sites used in the analysis, shown as blue dots.

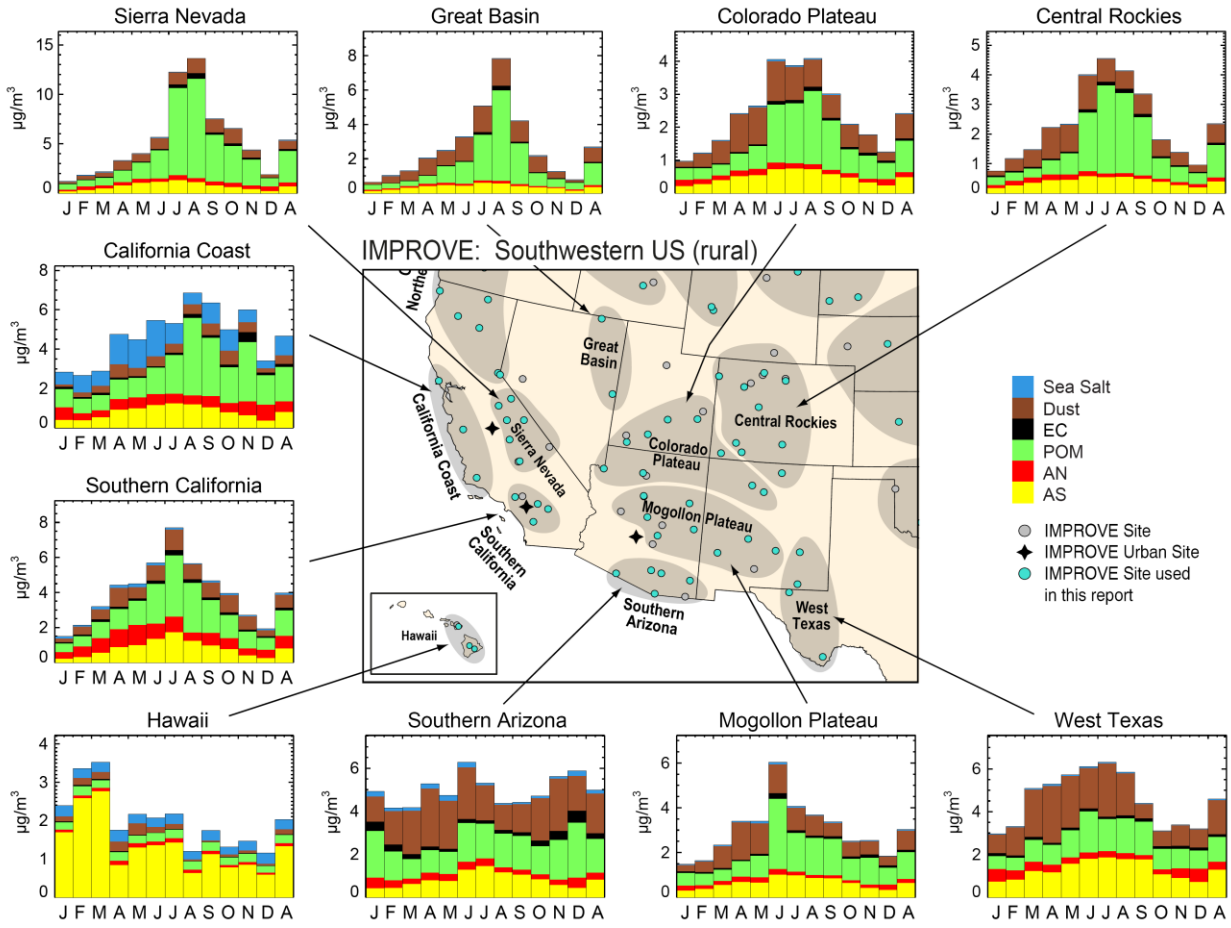

Figure S.4.3. IMPROVE 2016–2019 regional monthly mean $PM_{2.5}$ mass concentrations (µg m^{-3}) for the southwestern United States. Letters on the x-axis correspond to month and "A" corresponds to annual mean. Shaded areas in the map correspond to regions that include the sites used in the analysis, shown as blue dots.

Similar to the IMPROVE regions, in CSN regions AS monthly mean concentrations in the eastern United States rarely reached above 2 µg m^{-3} (see Figure S.4.4). The similarity in seasonal patterns of AS concentrations in the eastern United States pointed to regional sources of AS that influence both urban and rural regions. In addition, the seasonal variability was low, with mostly flat monthly mean concentrations year round. Monthly mean AS concentrations were generally low (<1.5 µg m^{-3}) for CSN regions in the northwestern United States (Figure S.4.5) and were seasonally flat, similar to IMPROVE monthly mean concentrations. The exception was the Alaska region, with maximum monthly mean concentrations during cold months. The regional monthly mean AS concentrations in the southwestern United States were generally low (<2.0 µg m^{-3}) in most regions but with more seasonal variability than in the eastern United States (Figure S.4.6). Summer maxima were observed for many regions, such as in the Phoenix/Tucson, Albuquerque, Las Vegas, and West Texas regions. The strongest seasonal variability occurred in the Los Angeles and San Diego regions with summer maxima. These patterns also occurred for IMPROVE regions. The Hawaii region experienced some seasonal variability with winter maxima.

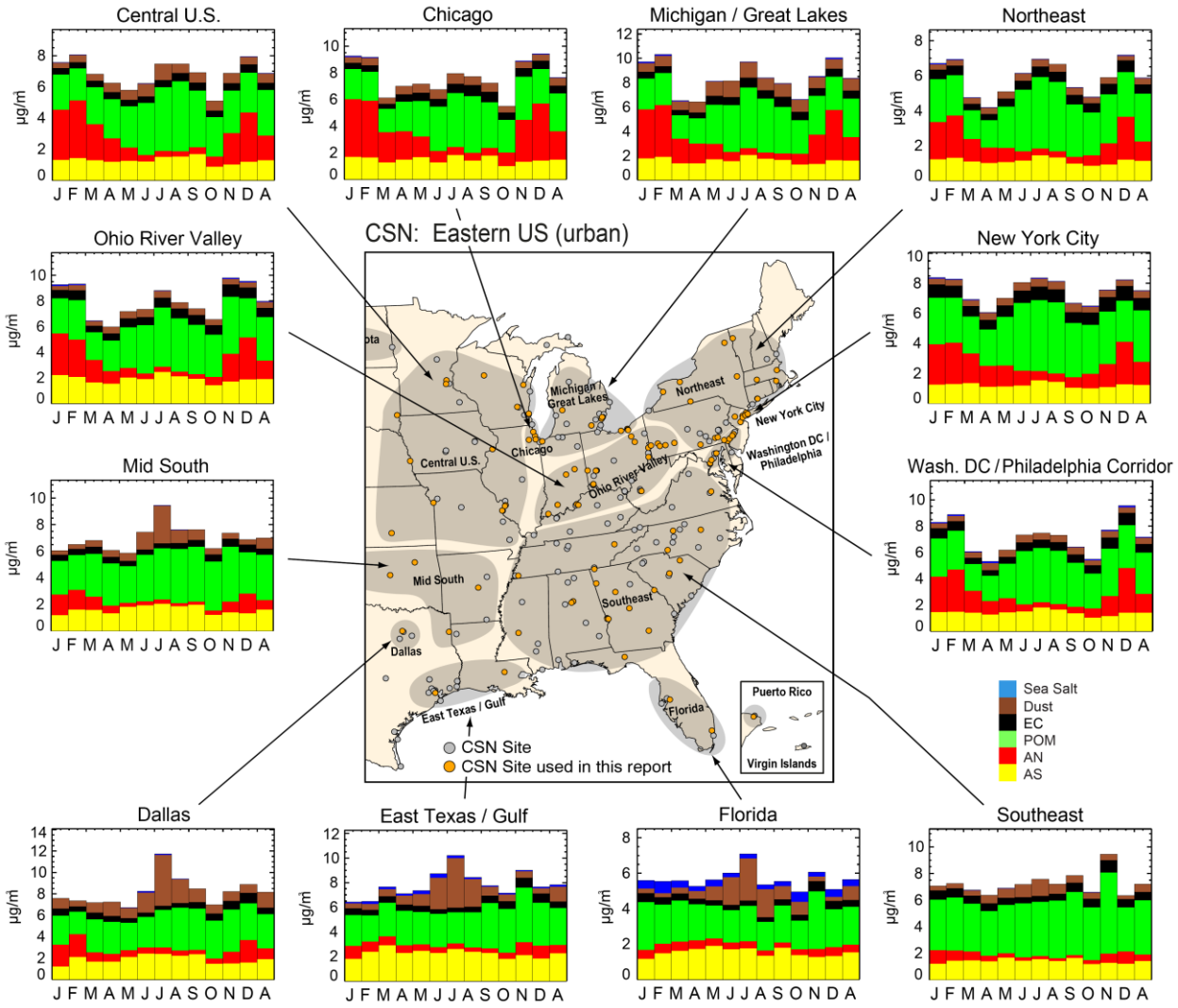

Figure S.4.4. CSN 2016–2019 regional monthly mean $PM_{2.5}$ mass concentrations (µg m^{-3}) for the eastern United States. Letters on the x-axis correspond to month and "A" corresponds to annual mean. Shaded areas in the map correspond to regions that include the sites used in the analysis, shown as orange dots.

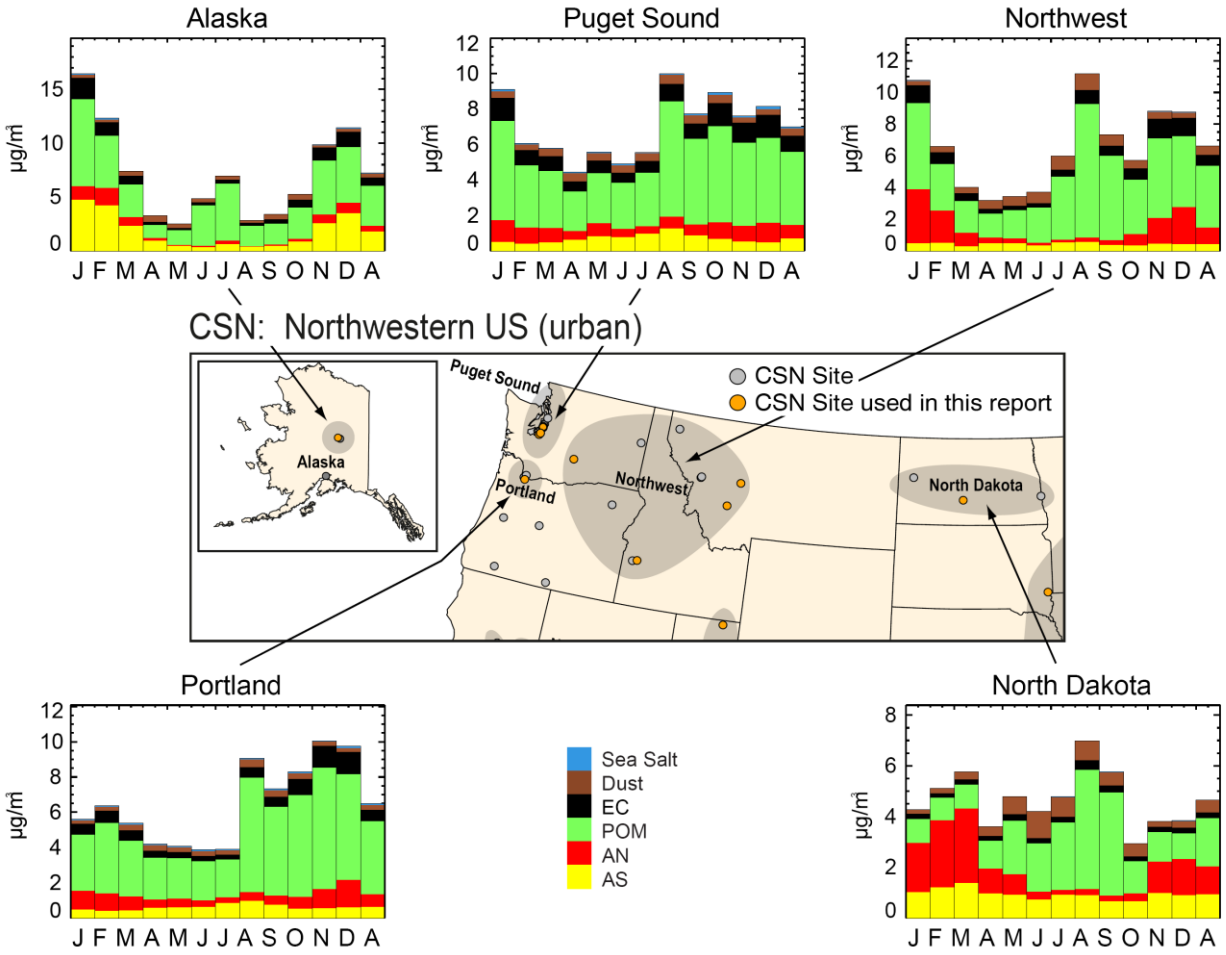

Figure S.4.5. CSN 2016–2019 regional monthly mean $PM_{2.5}$ mass concentrations (μg m^{-3}) for the northwestern United States. Letters on the x-axis correspond to month and "A" corresponds to annual mean. Shaded areas in the map correspond to regions that include the sites used in the analysis, shown as orange dots.

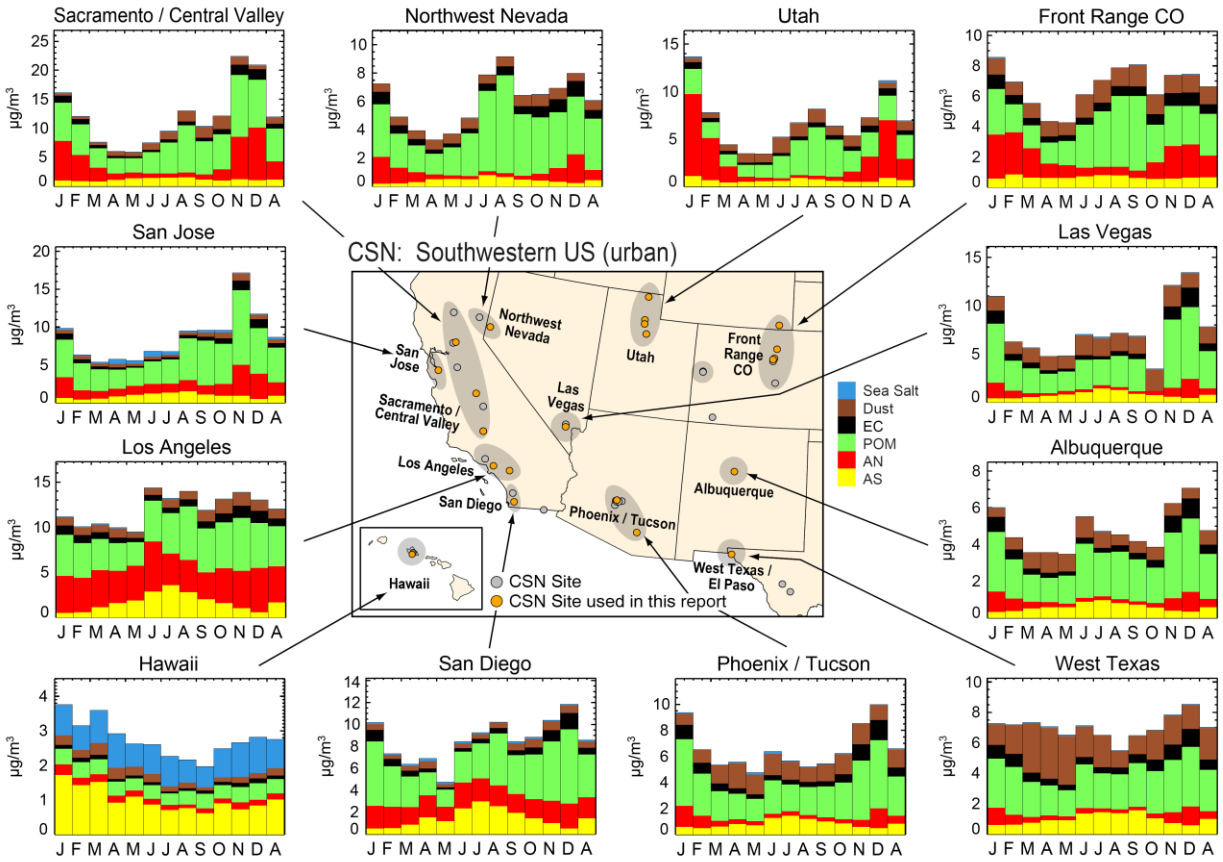

Figure S.4.6. CSN 2016–2019 regional monthly mean $PM_{2.5}$ mass concentrations (µg m^{-3}) for the northwestern United States. Letters on the x-axis correspond to month and "A" corresponds to annual mean. Shaded areas in the map correspond to regions that include the sites used in the analysis, shown as orange dots.

S.4.2 Ammonium Nitrate

In the eastern United States, the highest IMPROVE AN monthly mean concentrations occurred during winter months in the Central Great Plains region, near 3 µg m^{-3} (Figure S.4.1). Along with the Central Great Plains region, winter monthly mean concentrations were generally higher for regions farther north with mean concentrations nearing 2 µg m^{-3}. Farther south, regional mean concentrations were much lower (<1 µg m^{-3} year round). In the northwestern United States, the highest monthly mean concentrations occurred during winter months in the Columbia River Gorge and Northern Great Plains regions (Figure S.4.2). Other regions in the northwestern United States experienced relatively low concentrations year round (<0.3 µg m^{-3}). Regions in the southwestern United States also had low concentrations (Figure S.4.3). The exceptions were the California Coast and Southern California regions, where concentrations were higher (<1 µg m^{-3}). Unlike regions in the eastern United States, regions in the northwestern and southwestern United States had low monthly variability, and, interestingly, the AN monthly mean concentrations in the Southern California region peaked in spring.

In the eastern United States, a strong seasonal pattern in monthly mean AN was observed for CSN regions, with peaks in winter months, especially for regions farther north (Figure S.4.4). High concentrations (~4 µg m^{-3}) occurred in winter months in the Central U.S. and

Michigan/Great Lake regions. Concentrations decreased for regions farther south, with lower monthly variability. A similar spatial pattern was observed for IMPROVE regions. Concentrations were generally lower for regions in the northwestern United States (Figure S.4.5). The Northwest and North Dakota regions had the highest monthly mean concentrations near 3 $\mu g\ m^{-3}$ during winter months. Regions in the southwestern United States experienced the highest monthly mean concentrations (see Figure S.4.6). Mean concentrations decreased in regions farther south, such as in the Las Vegas, Albuquerque, West Texas, and Phoenix/Tucson regions, although maxima still occurred in winter months. In contrast, regions in southern California, such as Los Angeles and San Diego, experienced higher concentrations year round.

S.4.3 Particulate Organic Matter

In the eastern United States, IMPROVE POM monthly, regional mean concentrations were highly seasonal, with peaks in summer months (Figure S.4.1). During July and August, concentrations reached over 3 $\mu g\ m^{-3}$ in most regions. The strong peak in POM in April in the Southeast region was due to the influence of biomass smoke. The largest regional mean POM concentrations occurred in the northwestern United States (Figure S.4.2) where peak concentrations ranged from 5 to 12 $\mu g\ m^{-3}$, mainly in August and September due to biomass smoke influence. A strong seasonal pattern in POM was observed at these regions, with relatively low concentrations during winter months (<1 $\mu g\ m^{-3}$). This pattern was also observed for more-northerly regions in the southwestern United States (Figure S.4.3), but the magnitude of the concentrations and degree of seasonality decreased farther south.

CSN POM monthly mean concentrations in regions in the eastern United States ranged from 2 to 5 $\mu g\ m^{-3}$ and peaked during summer months in many regions farther north (Figure S.4.4). Toward the south, regions had less seasonal variability; however, magnitudes of POM were similar. Higher concentrations were observed in regions in the northwestern United States, likely associated with biomass smoke impacts (Figure S.4.5). The Northwest, Portland, and North Dakota regions experienced monthly mean concentrations of 6–8 $\mu g\ m^{-3}$, especially during summer and fall months. In the southwestern United States, regions toward the north also experienced high POM concentrations during summer and fall, such as the Northwest Nevada, Sacramento/Central Valley, San Jose, and Front Range CO regions (Figure S.4.6). Farther south, POM concentrations peaked during winter months, such as in the Albuquerque, Phoenix/Tucson, and West Texas regions.

S.4.4 Elemental Carbon

IMPROVE EC regional mean concentrations are difficult to discern on the bar charts because they are low relative to other aerosol species. In the eastern United States, concentrations rarely exceeded 0.3 $\mu g\ m^{-3}$ (Figure S.4.1). Unlike other species, the monthly variability of EC was highly spatially variable. The Boundary Waters region peaked during summer months, Central Great Plains during spring months, Ohio River Valley during fall and winter months, Appalachia during fall months, and in the Southeast during spring and fall months. The monthly mean seasonal and spatial variability suggests localized impacts of sources in regions in the eastern United States. In contrast, monthly mean concentrations in regions in the northwestern United States peaked in late summer and/or early fall for all of the regions (Figure

S.4.2). Concentrations were >0.5 μg m^{-3} in the Hells Canyon, Northern Rockies, Northwest, and Oregon/Northern California regions in August or September, indicating the important role of biomass burning in the area. Lower monthly mean EC concentrations were also observed in regions in the southwestern United States (Figure S.4.3) in summer, except in the Sierra Nevada region in August (~0.5 μg m^{-3}) and in the California Coast region in November (~0.5 μg m^{-3}). Farther south, concentrations peaked during winter months in the Southern Arizona region (~0.5 μg m^{-3} in December). Otherwise, monthly mean concentrations in most regions rarely exceeded 0.2 μg m^{-3}.

CSN EC monthly mean concentrations in the eastern United States peaked between 0.5 and 1.0 μg m^{-3} and were higher in regions such as the Ohio River Valley, Chicago, and New York City regions (Figure S.4.4). Concentrations were generally low in regions farther south, with the exception of the Dallas and Southeast regions, where concentrations almost reached 1 μg m^{-3} during cold months. Monthly mean concentrations were generally higher in regions in the northwestern United States than in the eastern United States. Concentrations reached over 1.0 μg m^{-3} during fall and winter months, such as in the Puget Sound, Northwest, and Portland regions (Figure S.4.5). In some southwestern regions, monthly mean concentrations also reached values over 1.0 μg m^{-3}, such as the Sacramento/Central Valley, San Diego, Los Angeles, Northwest Nevada, Phoenix/Tucson, and Albuquerque regions, often during late fall (Figure S.4.6).

S.4.5 Fine Dust Mass

The seasonal and spatial variability of FD in the United States is influenced by local, regional, and long-range transport. A maximum 2016–2019 regional monthly mean IMPROVE FD mass concentration of 4.01 μg m^{-3} was observed in August in the Virgin Islands region, a site known to have impacts from North African dust transport, especially during summer (Figure S.4.1). In the eastern United States, the highest FD concentration occurred during summer months, especially at regions farther south, such as the Southeast and Midsouth regions (>2.0 μg m^{-3}). Concentrations during winter months were relatively low (0.1–0.3 μg m^{-3}). Monthly mean FD concentrations in the northwestern United States were highest in the Columbia River Gorge region in summer (Figure S.4.2). Monthly mean concentrations in other regions were relatively low (<1 μg m^{-3}) but also peaked during summer months. Regional mean concentrations in the southwestern United States were highest (2–3 μg m^{-3}) for regions farther south (Figure S.4.3) and peaked in spring and early summer months. Regions farther north, such as the Sierra Nevada and Great Basin regions, had higher concentrations during summer and fall months.

CSN regions farther south in the eastern United States had higher FD concentrations in summer months, such as in the Dallas and East Texas/Gulf regions (4–5 μg m^{-3} in July) and the Midsouth and Florida regions (2–3 μg m^{-3} in July), likely associated with long-range transport of North African dust. Monthly mean concentrations in other eastern CSN regions ranged between 0.5 and 1.0 μg m^{-3} (Figure S.4.4). In the northwestern United States, monthly mean concentrations were typically <0.5 μg m^{-3} in most regions year round. The exception was in the Northwest region, where concentrations reached over 1.0 μg m^{-3} in August, and the North Dakota region in June (Figure S.4.5). Relatively high concentrations (1–3 μg m^{-3}) were observed in many regions in the southwestern United States (Figure S.4.6) during spring months. Monthly

mean concentrations in the Sacramento/Central Valley region reached over 2 μg m^{-3} during fall months, and in the Los Angeles region monthly mean concentrations were over 1 μg m^{-3} during April and fall months.

S.4.6 $PM_{2.5}$ Sea Salt

Estimates of SS discussed here are likely an underestimate, as chloride concentrations in the particle phase can be depleted by a gas–particle exchange of chloride to the atmosphere. IMPROVE regional mean SS concentrations were visible on the monthly bar charts relative to other species for only a few regions. In the eastern United States, coastal regions such as the Northeast, East Coast, and Southeast regions had noticeable SS concentrations relative to other species (Figure S.4.1). In the East Coast and Southeast regions, concentrations reached 0.7 μg m^{-3} in the late winter and spring months. In the northwestern United States, monthly mean SS concentrations neared 0.2 μg m^{-3} in the Columbia River Gorge and Northwest regions in April (Figure S.4.2), but in other regions, concentrations were typically <0.02 μg m^{-3}. In the Alaska region, monthly mean SS concentrations reached 0.7 μg m^{-3} in February. In the southwestern United States, regional mean SS concentrations were higher in the California Coast and Hawaii regions (Figure S.4.3).

CSN regional mean SS concentrations were relatively low and difficult to discern on the bar charts corresponding to regions in the eastern United States (Figure S.4.4), with the exception of the Florida and East Texas/Gulf regions. Monthly mean SS concentrations in the regions in the northwestern United States were quite low, generally around 0.1 μg m^{-3} or less (Figure S.4.5). Regions in the southwestern United States were also associated with low SS regional mean concentrations (Figure S.4.6). The San Jose and Hawaii regions had some of the highest monthly mean concentrations.

S.4.7 $PM_{2.5}$ Gravimetric Fine Mass

Regional monthly mean FM concentrations mirrored the combined species concentrations on the bar charts shown in previous figures in this section. IMPROVE regional monthly mean concentrations in the eastern United States peaked during summer, around 6–8 μg m^{-3}. The highest monthly mean concentrations occurred during summer in the Midsouth and Ohio River Valley regions. The Southeast region was influenced by biomass smoke during April, when POM concentrations increased over other months. In the northwestern United States, strong seasonal variability due to the impacts of biomass smoke and increased POM concentrations led to peaks in FM in the Northwest, Northern Rockies, Hells Canyon, and Oregon/Northern California regions, over 12 μg m^{-3}. Biomass smoke impacts also influenced FM concentrations in regions in the southwestern United States, such as the Sierra Nevada region in July and August, when FM was over 10 μg m^{-3}. Summer peaks in FM also occurred in many other southwestern regions but at lower concentrations (~6–8 μg m^{-3}).

Regional, monthly mean CSN FM concentrations peaked in both winter and summer in several northern regions in the eastern United States. Farther south, FM concentrations peaked in summer and were flatter during winter months. Monthly mean FM peaked in both summer and winter at regions in the northwestern United States and reached values near 10 μg m^{-3}. Similar

seasonal patterns in monthly mean FM occurred in regions in the southwestern United States. FM monthly mean concentrations in the West Texas region were relatively flat, while concentrations in the Phoenix/Tucson region peaked during winter. In the Los Angeles region, monthly mean concentrations for the first half of the year were relatively low and increased in June for the rest of the year.

S.4.8 Discussion

The differences observed in the seasonal and spatial patterns in species concentrations for the rural regions of the IMPROVE network and the urban/suburban regions in the CSN network were indicative of the spatial extent of aerosol sources, atmospheric processes, regional transport, and sinks. For example, regional mean AS seasonal patterns and concentrations were similar for both the IMPROVE and CSN regions. In the eastern United States, monthly mean AS concentrations were similar in magnitude and had low monthly variability in both urban and rural regions. For nearly all urban and rural regions, monthly mean concentrations were near 2 $\mu g\ m^{-3}$ or less and fractional contributions were <0.3. Concentrations in urban and rural regions in the northwestern United States were lower (<2 $\mu g\ m^{-3}$) than in regions in the eastern United States, likely due to lower emissions of SO_2. The variability of monthly mean AS concentrations was more pronounced in rural regions compared to urban regions in the northwestern United States, in part because of the large contributions from POM during summer. Some urban regions also exhibited this pattern. Contributions of AS to RCFM in northwestern U.S. regions were typically <0.2, lower than for eastern U.S. regions. In urban CSN regions in the southwestern United States, AS concentrations peaked in summer at many regions. Less monthly variability was seen in rural IMPROVE regions; however, similar magnitudes in concentration were observed.

Seasonal and spatial patterns in monthly mean AN concentrations were similar between urban and rural regions. For example, in the eastern United States, monthly mean concentrations were higher in regions farther north that were closer to areas with extensive agricultural activity, such as the Midwest United States. However, AN concentrations were higher in urban regions. Concentrations peaked during winter months in both urban and rural regions, and often exceeded AS concentrations. Monthly variability and concentration magnitude decreased for regions farther south for both urban and rural regions. Contributions were a significant fraction of RCFM in urban and rural regions, especially during winter months in regions farther north. AN monthly mean concentrations were lower in regions in the northwestern United States, although concentrations in urban regions were still higher than in rural regions. Higher monthly mean concentrations were observed during winter months near areas of agricultural activity for both urban and rural regions. AN concentrations were higher than AS concentrations during winter months in many urban and rural regions in the northwestern United States. In the southwestern United States, higher urban mean AN concentrations were observed relative to rural regions, especially in California, Utah, and Colorado.

The strong summer maxima in regional mean POM concentrations in western IMPROVE regions suggested that wildfire activity was a major contributor to POM concentrations in rural areas, especially in the western and northwestern United States in summer. Biogenic secondary organic aerosol also could have contributed significantly to high summer POM concentrations.

Urban regions experienced maxima in monthly mean POM concentrations during summer but also during winter months, likely due to additional local sources and meteorological conditions. In regions in the southwestern United States, both summer and winter maxima were common in urban regions, whereas most rural regions experienced maxima during summer. Seasonal and spatial variability in rural and urban regions were similar in the eastern United States, with higher concentrations during summer months. Less monthly variability was observed in urban regions farther south, which was not reflected at rural regions. POM monthly mean concentrations in eastern U.S. urban regions were typically higher than at rural regions. POM was the dominant contributor to RCFM at all areas of the United States. In the eastern United States, half of RCFM was composed of POM in both urban and rural regions, especially during summer months. These contributions were greater in both urban and rural regions in the northwestern United States; contributions over 0.7 were common. The contributions decreased for southwestern U.S. regions, but during summer, POM could dominate RCFM at both urban and rural regions, and in some urban regions, POM could be equally important during winter months.

Monthly mean EC concentrations were higher in urban regions across the United States. The urban regional monthly mean maxima were nearly three times higher than those in rural regions. In rural regions, EC seasonal and spatial patterns tended to follow those of POM, especially in northwestern U.S. regions where biomass smoke impacts were significant sources. Summer maxima in monthly mean EC reflected smoke contributions, but higher winter contributions were also observed, especially in urban regions, likely due to residential heating. Contributions to RCFM were also higher in urban regions across the United States.

FD concentrations were influenced by both local and long-range transport. The long-range transport of North African dust influenced both urban and rural regions in the eastern United States during summer in regions farther south. This influence was especially evident in the relative contribution of FD to RCFM. Monthly mean FD concentrations were higher near agricultural areas for both urban and rural regions, such as the Central Great Plains/Central U.S. and Northern Great Plains. The spring dust phenomenon in the southwestern United States also influenced both rural and urban regions. Contributions of FD to RCFM were significant during spring months (~0.5), suggesting both local and regional sources influenced RCFM across the southwestern United States.

SS concentrations and fractional contributions were negligible in most urban and rural regions. Coastal regions (including regions on both the east and west coasts, including the Hawaii and Alaska regions) were the only regions to experience non-negligible impacts from SS on RCFM. SS corresponded to a high degree of seasonality.

FM concentrations were noticeably higher in urban regions than rural regions. The regional mean urban maximum was nearly twice that of rural maximum. The rural monthly mean maximum was likely due to the impact of biomass smoke, given its occurrence in the Oregon/Northern California region in August and the dominant role of POM. The maximum urban monthly mean FM concentration occurred in the Sacramento/Central Valley region in December due to POM and AN concentrations. For most urban and rural regions across the United States, depending on season, the highest FM concentrations occurred due to high

contributions of POM and AN, highlighting their importance to the FM budget, as well the roles of biomass smoke and agricultural influence.

S.5 SPATIAL AND SEASONAL PATTERNS IN RELATIVE RECONSTRUCTED AEROSOL LIGHT EXTINCTION COEFFICIENTS

Reconstructed total aerosol light extinction coefficients (b_{ext_tot}) were computed from speciated aerosol mass concentrations, multiplied by a species-specific extinction efficiency and a humidification factor (f(RH)), and summed over all species. The extinction algorithm used to compute b_{ext_tot} is shown in equation (S.5.1):

$$b_{ext\_tot} = 3\times f(RH)\times[AS] + 3\times f(RH)\times[AN] + 4\times[POM] + 10\times[EC] + 1\times[FD] + 1.7\times f(RH)_{ss}\times[SS] + 0.6\times[CM] + \text{site-specific Rayleigh scattering} \quad \text{(S.5.1)}$$

The units of b_{ext_tot} and Rayleigh scattering are in inverse megameters (Mm^{-1}). The same f(RH) curve was applied to AS and AN, while a separate f(RH) was applied to SS ($f(RH)_{SS}$, see Chapter 4.1). Mass concentrations of aerosol species (in brackets) are in $\mu g\ m^{-3}$, and mass scattering and absorption efficiencies have units of $m^2\ g^{-1}$. Values of 3 $m^2\ g^{-1}$ were used for both AS and AN, 4 $m^2\ g^{-1}$ for POM, 10 $m^2\ g^{-1}$ for EC, 1 $m^2\ g^{-1}$ for soil, 1.7 $m^2\ g^{-1}$ for SS, and 0.6 $m^2\ g^{-1}$ for CM. For CSN sites, CM was interpolated to CSN sites from nearby EPA FRM sites (see Chapter 4). Extinction values correspond to a wavelength of 550 nm.

Visual range and extinction measurements are nonlinear with respect to human perception of visual scene changes caused by haze. The deciview (dv) haze index was derived with a number of assumptions such that uniform changes in haze correspond to approximately uniform incremental changes in visual perception (Pitchford and Malm, 1994). Deciview is calculated from reconstructed b_{ext_tot}, using equation (S.5.2):

$$dv = 10\times\ln(b_{ext\_tot}/10) \quad \text{(S.5.2)}$$

For different values of site-specific Rayleigh scattering, as specified in equation (S.5.1), it is possible to have a negative dv for pristine conditions (b_{ext_tot} <10 Mm^{-1}).The spatial variability in dv and b_{ext_tot} are similar to the spatial variability in aerosol mass concentrations; however, because of relative humidity (RH) effects and different mass extinction efficiencies, the relative contributions from individual species to b_{ext_tot} may be different than their contributions to reconstructed fine mass. Because of the similarity between aerosol speciated mass and b_{ext_tot}, only annual mean b_{ext_tot} and dv are discussed in Section S.5.1 (see Chapter 4 for individual species).

Regional, monthly mean reconstructed b_{ext_tot} and speciated extinction values were computed for the major aerosol species listed earlier and for similar regions discussed in Section S.4 and Chapters 3 and 5. Seasonal patterns of speciated extinction are similar to those for mass, so only the relative contribution of major aerosol species to b_{ext_aer} (b_{ext_tot} – Rayleigh scattering) are shown in Section S.5.2–S.5.8. See Chapter 5 for additional details.

S.5.1 Annual Mean Reconstructed Light Extinction Coefficient

The 2016–2019 IMPROVE annual mean b_{ext_tot} is presented in Figure S.5.1a. The east–west gradient observed for several species (especially AS) was preserved in the calculation of b_{ext_tot}, but sites with the highest b_{ext_tot} were in the central United States due to agricultural activity and in Florida due to biomass smoke impacts. Sites with the lowest b_{ext_tot} occurred in the southwestern United States and the Intermountain West. Higher b_{ext_tot} occurred at sites in California and the northwestern United States.

The addition of CSN sites preserved the large-scale gradients observed with IMPROVE sites, with higher b_{ext_tot} in the central and eastern United States compared to lower estimates at sites in the Intermountain West and southwestern United States (Figure S.5.1b). The addition of sites in the eastern United States provided further resolution that focused the area of high b_{ext_tot} (>50 Mm^{-1}) in the central United States, especially at sites in Indiana and Pennsylvania. High b_{ext_tot} also occurred at sites in Texas and at Gulf sites (>50 Mm^{-1}) and along the Central Valley of California.

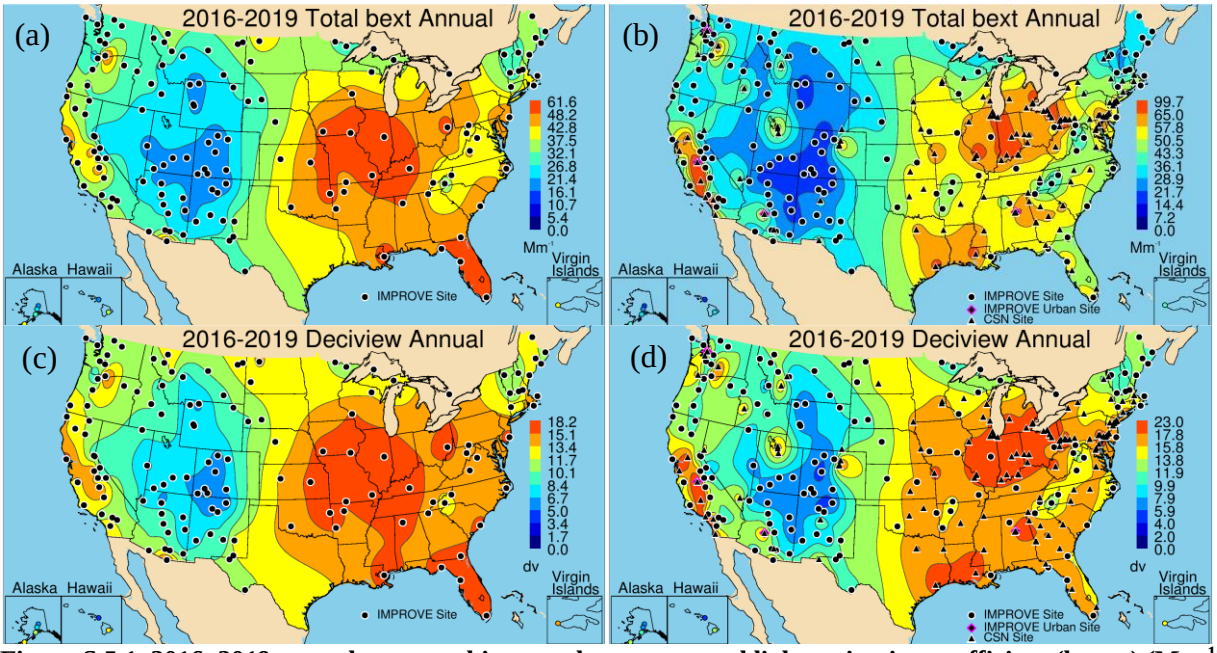

Figure S.5.1. 2016–2019 annual mean ambient total reconstructed light extinction coefficient (b_{ext_tot}) (Mm^{-1}) for (a) IMPROVE and (b) IMPROVE and CSN. Annual mean deciview (dv) for (c) IMPROVE and (d) IMPROVE and CSN. Wavelength corresponds to 550 nm.

The 2016–2019 IMPROVE annual mean dv spatial pattern was very similar to the b_{ext_tot} pattern, as expected (see Figure S.5.1c). Higher dv values (>15 dv) were observed at sites in the eastern United States, with the exception of northeastern sites (10–11 dv). Lower values were observed at sites in the Intermountain West, especially at sites in the central Rocky Mountains of Colorado and northern New Mexico. Higher estimates were observed at sites in California (~15).

Similar to the map of b_{ext_tot}, the addition of urban sites to the dv map in Figure S.5.1d provided additional spatial resolution but did not change the overall patterns. The highest annual mean dv occurred at sites in the central United States and the Gulf area, as well as at sites in the Central Valley of California. Additional hot spots included sites in Colorado, Utah, Arizona, and Nevada.

S.5.2 Ammonium Sulfate Light Extinction Coefficients

The largest IMPROVE fractional contribution from b_{ext_AS} to b_{ext_aer} (~0.5) occurred in the Ohio River Valley and Appalachia regions. Other regions in the eastern United States corresponded to maximum monthly mean fractions around 0.4–0.45 that occurred mostly during summer and early fall months (Figure S.5.2). The seasonality of the fractional contribution of b_{ext_AS} to b_{ext_aer} in regions in the northwestern United States differed from that observed for eastern regions, with minima in b_{ext_AS} contributions in summer months, largely due to the strong contributions from b_{ext_POM} during summer (Figure S.5.3). The seasonality of the fractional contribution of b_{ext_AS} to b_{ext_aer} in regions farther north in the southwestern United States followed those of the northwestern region, with lower contributions that occurred in the summer months due to the role of b_{ext_POM} contributions (Figure S.5.4). Contributions of b_{ext_AS} in regions farther south tended to have flat seasonality, or summer/early fall maxima.

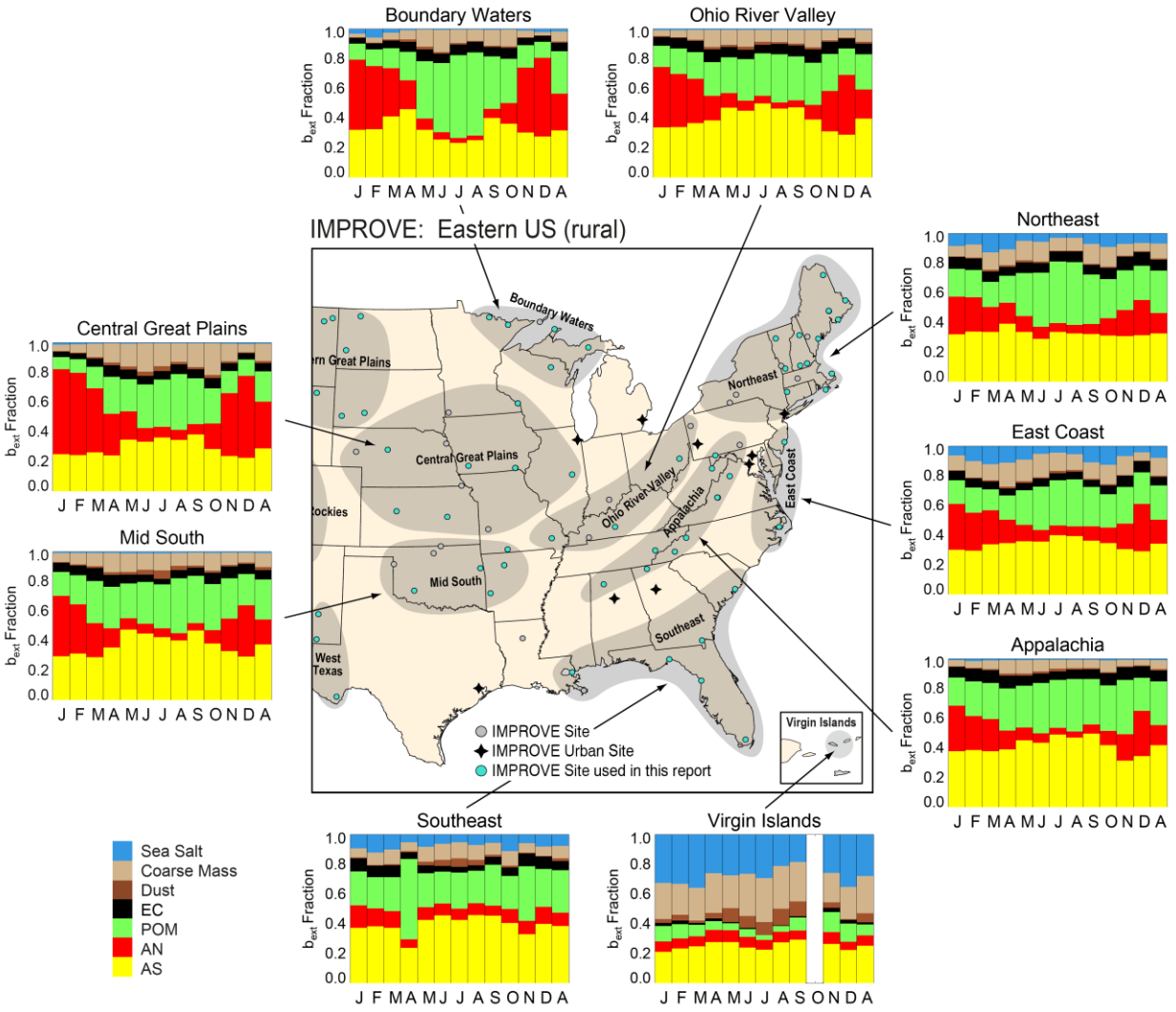

Figure S.5.2. IMPROVE 2016–2019 regional monthly mean speciated fractional contributions to ambient aerosol light extinction coefficients (b_{ext}) for the eastern United States. Letters on the x-axis correspond to the month and "A" corresponds to annual mean. Shaded areas in the map correspond to regions that include sites used in the analysis, shown as blue dots. Wavelength corresponds to 550 nm.

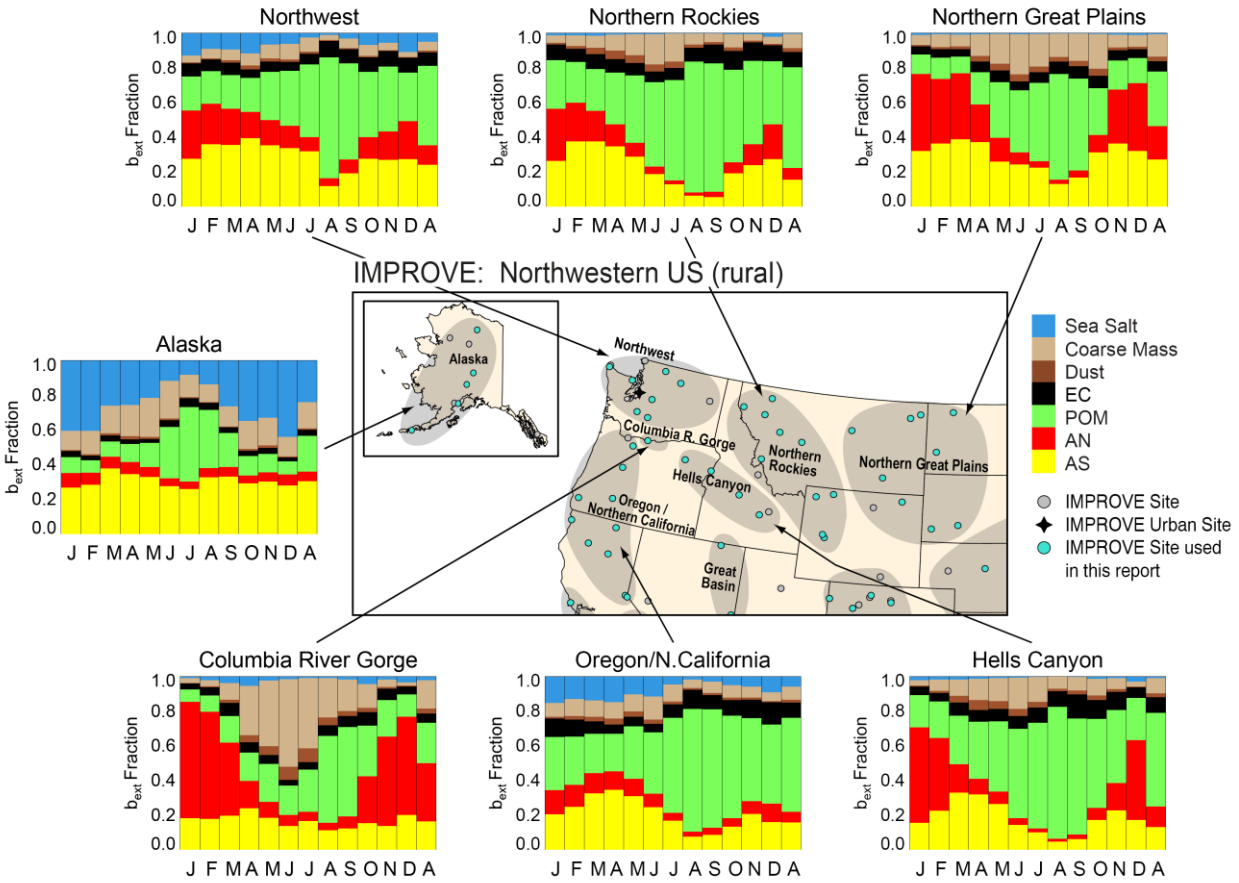

Figure S.5.3. IMPROVE 2016–2019 regional monthly mean speciated fractional contributions to ambient aerosol light extinction coefficients (b_{ext}) for the northwestern United States. Letters on the x-axis correspond to the month and "A" corresponds to annual mean. Shaded areas in the map correspond to regions that include sites used in the analysis, shown as blue dots. Wavelength corresponds to 550 nm.

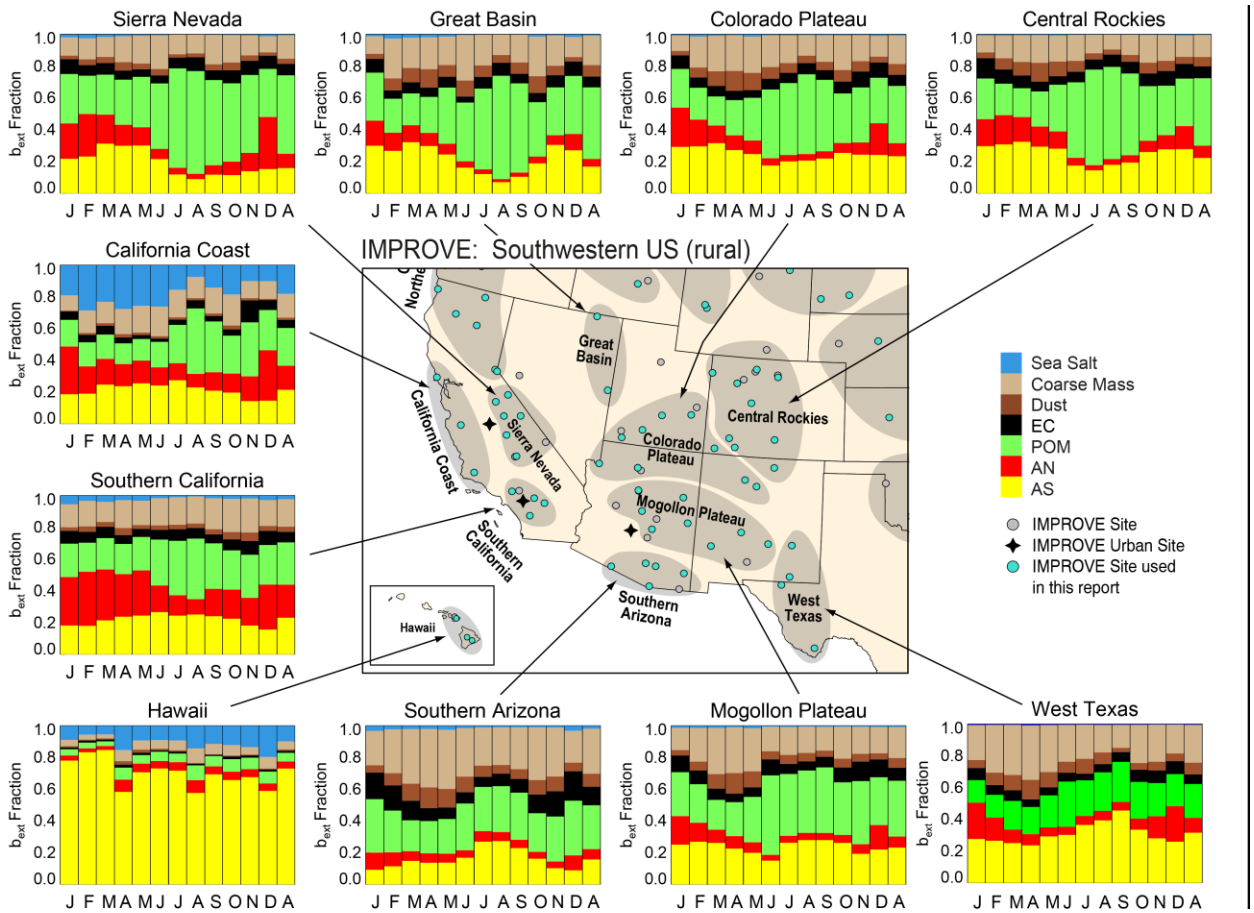

Figure S.5.4. IMPROVE 2016–2019 regional monthly mean speciated fractional contributions to ambient aerosol light extinction coefficients (b_{ext}) for the southwestern United States. Letters on the x-axis correspond to the month and "A" corresponds to annual mean. Shaded areas in the map correspond to regions that include sites used in the analysis, shown as blue dots. Wavelength corresponds to 550 nm.

The maximum contributions of b_{ext_AS} to b_{ext_aer} at CSN regions in the eastern United States were typically around 0.3-0.4 in summer and early fall months (Figure S.5.5). The lowest contributions were around 0.2-0.3 in winter months, lending to low seasonal variability in b_{ext_AS} contributions in regions in the eastern United States. While the seasonal patterns were quite similar across regions, the maximum contributions occurred in regions farther south. The relative contribution of b_{ext_AS} to b_{ext_aer} decreased considerably in regions in the western United States. Minimum b_{ext_AS} contributions in regions in the northwestern United States were around 0.1 (Figure S.5.6). The maximum contributions for these regions reached 0.2–0.3. Contributions were also relatively flat. Monthly mean contributions of b_{ext_AS} to b_{ext_aer} were lowest in regions in the southwestern United States relative to other areas of the country (Figure S.5.7). Minimum contributions were below 0.1, and maximum contributions were around 0.2–0.3, with the highest contribution in the San Diego region in July. A stronger seasonal variability occurred at regions in the southwestern United States relative to other regions, with summer maximum contributions common, especially in regions farther south.

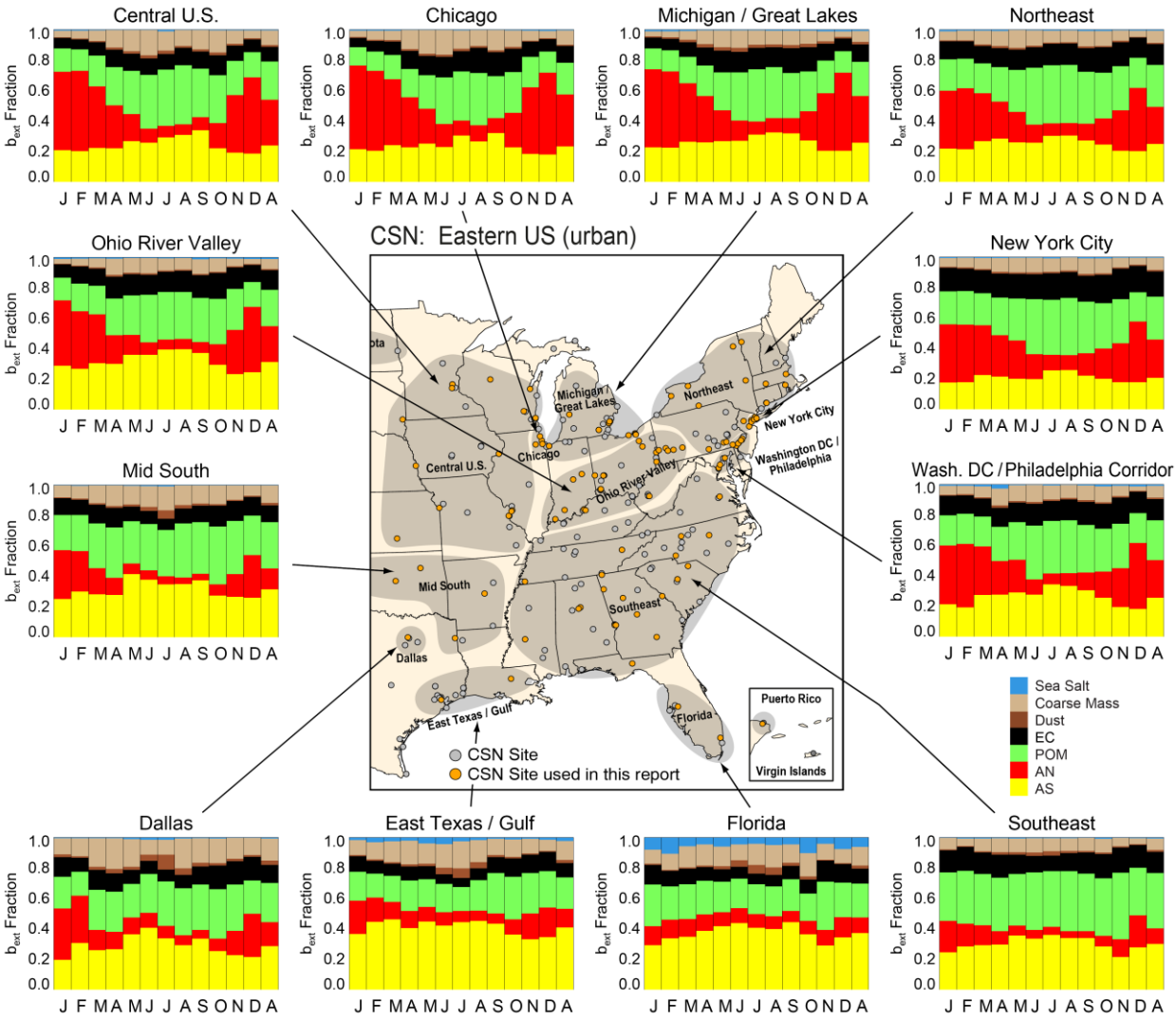

Figure S.5.5. CSN 2016–2019 regional monthly mean speciated fractional contributions to ambient aerosol light extinction coefficients (b_{ext}) for the eastern United States. Letters on the x-axis correspond to the month and "A" corresponds to annual mean. Shaded areas in the map correspond to regions that include sites used in the analysis, shown as orange dots. Wavelength corresponds to 550 nm.

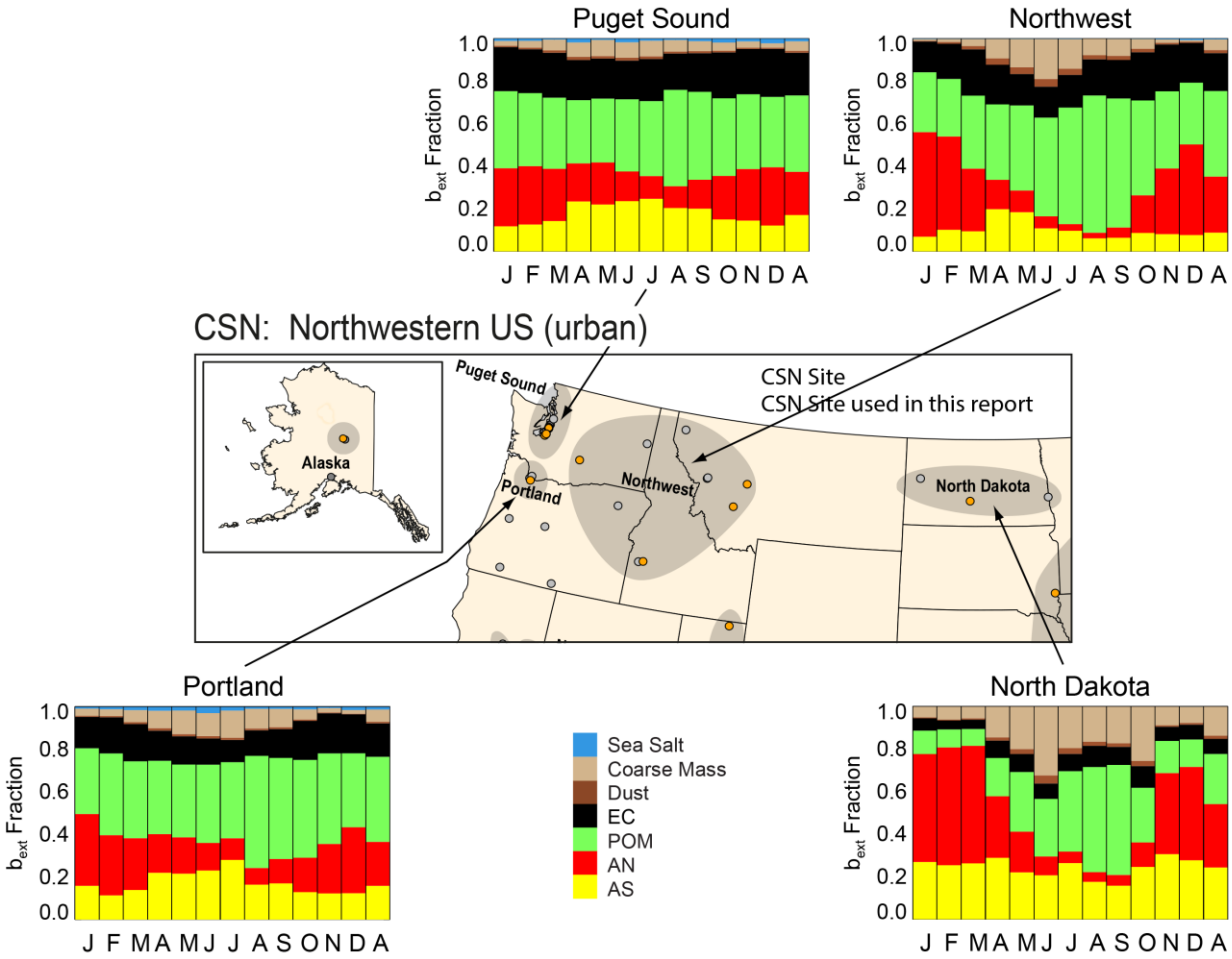

Figure S.5.6. 2016–2019 regional monthly mean speciated fractional contributions to ambient aerosol light extinction coefficients (b_{ext}) for the northwestern United States. Letters on the x-axis correspond to the month and "A" corresponds to annual mean. Shaded areas in the map correspond to regions that include sites used in the analysis, shown as orange dots. Wavelength corresponds to 550 nm.

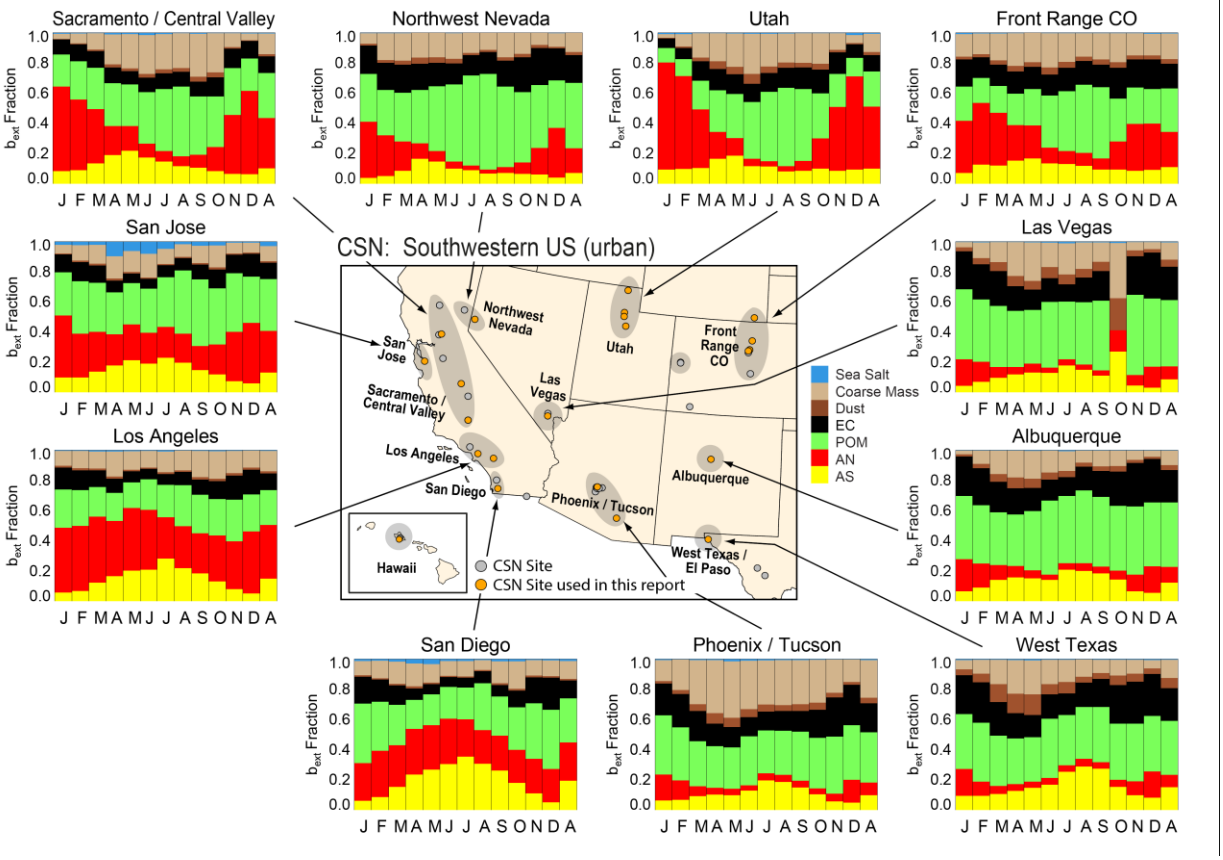

Figure S.5.7. CSN 2016–2019 regional monthly mean speciated fractional contributions to ambient aerosol light extinction coefficients (b_{ext}) for the southwestern United States. Letters on the x-axis correspond to the month and "A" corresponds to annual mean. Shaded areas in the map correspond to regions that include sites used in the analysis, shown as orange dots. Wavelength corresponds to 550 nm.

S.5.3 Ammonium Nitrate Light Extinction Coefficients

The contribution of b_{ext_AN} to b_{ext_aer} at IMPROVE regions farther north in the eastern United States experienced a high degree of seasonality (Figure S.5.2), for example contributions during summer months were around 0.03–0.06, compared to over 0.5 during winter months. Regions farther from agricultural sources, such as the East Coast, Northeast, and Appalachia regions, had lower maximum monthly mean contributions (~0.3 or less) in winter months. Regions farther south, such as the Southeast region, had the lowest year-round monthly mean contributions, ranging from 0.06 to 0.15. In the northwestern United States, the monthly mean contributions of b_{ext_AN} to b_{ext_aer} ranged from a minimum of 0.030 during summer months to 0.5–0.7 in winter months (Figure S.5.3). The regions with higher contributions were closer to agricultural activity and oil and gas development. Contributions in other regions, such as the Northern Rockies and Northwest regions, reached nearly 0.3 in winter. The relative contribution of b_{ext_AN} to b_{ext_aer} was lower in the southwestern United States relative to other areas (Figure S.5.4). Monthly mean contributions ranged from ~0.02 to 0.30 in summer and winter months, respectively.

CSN regional monthly mean b_{ext_AN} fractional contributions of b_{ext_AN} to b_{ext_aer} in the eastern United States were highest in regions farther north (Figure S.5.5), similar to IMPROVE regions. During winter months in the Central U.S., Chicago, and Michigan Great Lakes regions, b_{ext_AN} contributed over half of b_{ext_aer} and decreased to less than 0.1 during summer months. The range in seasonal contributions was much lower in regions farther south, where monthly mean contributions ranged from ~0.05 in summer months to ~0.2 or less during winter months. Regions in the southwestern United States experienced a strong seasonal contribution from b_{ext_AN} to b_{ext_aer}. For example, contributions in the North Dakota region ranged from 0.05 to 0.55 from summer to winter months (Figure S.5.6). High levels of contributions occurred in some southwestern U.S. regions. The Utah region had the highest monthly mean contribution in winter months of ~0.7 (Figure S.5.7) but much lower contributions (~0.05) during summer months. Regions in California experienced less seasonality in b_{ext_AN} contributions suggesting additional urban sources during summer months. The lowest contributions occurred in regions farther south; these regions experienced higher monthly mean contributions in winter relative to summer but ranged from ~0.03 to ~0.2 or less.

S.5.4 Particulate Organic Matter Light Extinction Coefficients

While the patterns of b_{ext_POM} were the same as those of POM mass concentrations, its relative contribution to reconstructed b_{ext} was not because of the hygroscopic and optical properties of other species contributing to b_{ext}. In the eastern United States, the IMPROVE regional maximum monthly mean b_{ext_POM} contribution was ~0.3–0.5 (Figure S.5.2). The April maximum in the Southeast region corresponded to biomass smoke influence. Minimum contributions of b_{ext_POM} to b_{ext_aer} at southeast U.S. regions occurred mostly during winter months or early spring. Contributions of b_{ext_POM} to b_{ext_aer} were much higher for many northwestern U.S. regions relative to the eastern United States, and the maximum monthly mean contributions occurred in August for nearly all regions (Figure S.5.3). The b_{ext_POM} contributions ranged from 0.071 in the Columbia River Gorge (January) and Alaska (February) regions to 0.76 in the Hells Canyon region (August). For most regions, the maximum monthly mean contributions were over 0.7, highlighting the importance of biomass burning influence on b_{ext_aer} in these regions. In the southwestern United States, regions farther north were likely influenced by biomass smoke, similar to regions in the northwestern United States area (Figure S.5.4). Minimum monthly mean contributions were typically around 0.15–0.2 for other regions and occurred in early spring or late winter months. Maximum monthly mean contributions were lower farther south and ranged from 0.3 to 0.4. The maximum contribution in the Southern Arizona region occurred in December; other regions experienced maxima during summer months.

For CSN regions in the eastern United States, monthly mean contributions in the Southeast region were greater than 0.3 during all months (Figure S.5.5). In regions farther north, contributions were greater in the summer months, in part due to contributions of b_{ext_AN} to b_{ext_aer} during winter months. Nearly all regions experienced their lowest monthly mean b_{ext_POM} contributions (~0.12–0.3) during winter months. Months corresponding to maximum contributions varied depending on region but many occurred during summer months. In the northwestern United States, most of the maximum contributions occurred during summer months (~0.45–0.65), and with the exception of the North Dakota region, minimum contributions in

other regions were around 0.3 (Figure S.5.6). Both the Puget Sound and Portland regions experienced relatively flat contributions of b_{ext_POM} to b_{ext_aer} compared to the Northwest and North Dakota regions, highlighting the importance of b_{ext_POM} contributions during winter farther west. Contributions of b_{ext_POM} were significant in many southwestern urban regions (Figure S.5.7), ranging from 0.278 in Los Angeles (November) to 0.635 in the Northwest Nevada region in August. Regions farther north experienced maximum contributions during summer, in part due to the contributions of b_{ext_AN} during winter months, when b_{ext_POM} contributions were lowest. Farther south, maximum contributions around 0.4–0.5 occurred during summer months.

S.5.5 Elemental Carbon Light Extinction Coefficients

Contributions of b_{ext_EC} to b_{ext_aer} were less than 0.1 in all IMPROVE eastern regions (Figure S.5.2) and generally higher during fall and winter months. Contributions of b_{ext_EC} to b_{ext_aer} were higher in regions in the northwestern United States (Figure S.5.3). In the Oregon/Northern California and Hells Canyon region, monthly mean maximum contributions were ~0.13 in December and September, respectively. Minimum monthly mean contributions were around 0.05, meaning that contributions year round were greater than 0.05 in most northwestern U.S. regions. In the southwestern United States, the maximum monthly contribution occurred in the Southern Arizona region (0.185) in December (Figure S.5.4). Maximum contributions in remaining regions were around 0.1, mostly during winter months. Minimum contributions were around 0.05.

Monthly mean contributions of b_{ext_EC} to b_{ext_aer} were higher in CSN regions compared to IMPROVE regions. In the eastern United States, maximum contributions were around ~0.1 and higher, with a maximum contribution of 0.200 in the New York City region in November (Figure S.5.5). Maximum contributions occurred mostly in fall months. Minimum monthly mean contributions were greater than 0.06 for all regions. In the northwestern United States, CSN b_{ext_EC} contributions ranged from 0.042 in the North Dakota region in February to nearly 0.23 in the Puget Sound and Northwest regions in January and October, respectively (Figure S.5.6). The North Dakota region was an outlier in the northwestern United States, where contributions were generally greater than 0.1. Maximum monthly mean b_{ext_EC} contributions in the southwestern United States were less than 0.3, with the maximum in Las Vegas. Regions in California had lower maximum contributions compared to those regions farther east (Figure S.5.7).

S.5.6 Fine Dust Light Extinction Coefficients

IMPROVE maximum monthly mean contributions b_{ext_FD} to b_{ext_aer} in the eastern United States were negligible, less than 0.03 in most regions, except the Midsouth (0.060) and the Southeast (0.060) regions, both in July (Figure S.5.2), likely due to long-range transport of North African dust. In the northwestern United States, contributions of monthly mean b_{ext_FD} to b_{ext_aer} were highest (0.080) in the Columbia River Gorge region in July (Figure S.5.3). Maxima in other regions in the northwestern United States were around 0.02–0.05, nearly all in April. Monthly mean contributions of b_{ext_FD} to b_{ext_aer} in the southwestern United States were highest (0.130) in the Southern Arizona and West Texas regions in April (Figure S.5.4). Other regions had maximum contributions in April of ~0.1.

In the eastern United States, the maximum CSN b_{ext_FD} contribution occurred in the Dallas region (0.100) in July (Figure S.5.5). Similar to b_{ext_FD}, regions with the highest maximum b_{ext_FD} contributions (~0.05) occurred in regions influenced by North African dust transport (e.g., East Texas/Gulf, Midsouth, and Florida regions) in July. Contributions of b_{ext_FD} to b_{ext_aer} were insignificant in regions in the northwestern United States (Figure S.5.6). Monthly mean maximum contributions were less than 0.04 in all regions. The maximum monthly mean b_{ext_FD} contributions in the southwestern United States (~0.2) occurred in the Las Vegas region in October and the West Texas region in May. Other regions in California had low maximum contributions (<0.03), while regions farther south were closer to 0.05–0.07 during spring months (Figure S.5.7). Of all the urban regions, those in the southwestern United States corresponded to the highest contributions of b_{ext_FD} to b_{ext_aer}.

S.5.7 $PM_{2.5}$ Sea Salt Light Extinction Coefficients

IMPROVE coastal regions in the eastern United States corresponded to higher maximum monthly mean contributions (~0.1–0.2) of b_{ext_SS} to b_{ext_aer} (Figure S.5.2). Contributions in noncoastal regions in the eastern United States were less than 0.05. Contributions of b_{ext_SS} to b_{ext_aer} in the northwestern United States were also highest at coastal regions (0.1–0.2). In the other northwestern U.S. regions, the contributions were 0.03 or less year round (Figure S.5.3). Similar to other areas, the southwestern United States had the only significant contributions of b_{ext}_ss in coastal regions, such as the California Coast and Hawaii regions (Figure S.5.4).

In the eastern United States the only CSN regions with non-negligible contributions were the Florida region in February (0.104) and the East Texas/Gulf region in June (0.04). All other regions had maximum contributions of 0.01 or less (Figure S.5.5). The maximum b_{ext_SS} contribution in the northwestern United States was around 0.02 in the Puget Sound region in December and the Portland region in June (Figure S.5.6). In the southwestern United States, maximum monthly mean b_{ext_SS} values were ~0.1 or less (Figure S.5.7). The highest contribution occurred in the San Jose region in April (~0.1). Other regions had maxima of 0.01 or less and were not visible on the regional bar charts.

S.5.8 Coarse Mass Light Extinction Coefficients

CM concentrations are estimated routinely by the IMPROVE network, and EPA FRM networks were used to interpolate CM to CSN sites in order to calculate b_{ext_CM}, b_{ext_aer}, b_{ext_tot}, and dv at CSN sites (see Chapter 4). Therefore, estimates of b_{ext_CM} for the CSN have additional uncertainty. In the eastern United States, IMPROVE b_{ext_CM} contributions were lowest during winter months for all regions (Figure S.5.2), except the Southeast region (April) and the Virgin Islands region (November). The largest maximum monthly mean b_{ext_CM} contribution occurred in the Virgin Islands region (0.30), but in other regions contributions were around 0.1–0.2, with the Central Great Plains region having contributions of ~0.2 in October, perhaps associated with agricultural harvesting. Other contributions were highest during spring and fall months. In the northwestern United States, contributions from b_{ext_CM} were the highest in the Columbia River Gorge region (~0.5 in June). Other regions had maximum contributions around 0.13–0.18, all in June (Figure S.5.3). Minimum monthly mean contributions ranged from ~0.03-0.10. Minimum contributions occurred during summer months perhaps due to the strong contributions from b_{ext_POM} during summer months. Maximum monthly mean contributions in the southwestern U.S.

regions ranged from ~0.18 in the Central Rockies region in to ~0.4 in the Southern Arizona region in May (Figure S.5.4). Most of the regions had contributions around 0.2 or higher, such as the West Texas region (0.342 in April). For many regions in the southwestern United States, b_{ext_CM} was one of the top third contributors to b_{ext_aer}, along with b_{ext_AS} and b_{ext_POM}.

In CSN regions in the eastern United States, b_{ext_CM} contributions ranged from ~0.03 (Washington D.C./Philadelphia Corridor region in December) to ~0.2 (Dallas region) in April (Figure S.5.5). Most of the monthly mean maxima were around 0.1–0.2 across eastern regions, and most occurred in late spring to summer months. The maximum monthly mean b_{ext_CM} contributions in the northwestern United States were similar in magnitude (0.1–0.2), with the largest in the North Dakota region (Figure S.5.6). Other maxima also occurred in June and July. Lower contributions occurred during winter months, around 0.01–0.05. With the exception of the North Dakota region, contributions of b_{ext_CM} were generally similar to or less than contributions from b_{ext_EC}. Higher contributions of b_{ext_CM} to b_{ext_aer} were observed in the southwestern United States (Figure S.5.7). Maximum contributions ranged from ~0.2 in the San Jose region in June to ~0.4 in the Phoenix/Tucson region in May. Otherwise, contributions were 0.2–0.3 in most regions.

S.5.9 Discussion

The seasonal patterns in b_{ext_tot} corresponding to major aerosol species were similar to the seasonal distributions in mass concentrations presented in Chapter 3. This similarity was expected for most species because mass concentrations were converted to b_{ext}, with mass extinction efficiencies that essentially scaled the values to b_{ext}. However, for AS, AN, and SS, the conversion to b_{ext_tot} accounted for RH effects and hygroscopic growth that can be considerable in environments with high RH. No significant differences were observed between the seasonal distributions in mass compared to b_{ext_tot} (see Chapter 5). Occasionally, the season that corresponded to the majority of the maximum and minimum regional absolute b_{ext_tot} or relative b_{ext_tot} changed for many of the species examined here. In addition, some species that were important for their contributions to RCFM were less important in reconstructed b_{ext_aer} (e.g., FD), while others became more important (e.g., EC, POM, and hygroscopic species). Differences in urban and rural b_{ext_aer} were evident, especially in seasonal patterns. Many of the urban regions had maximum b_{ext_aer} during winter, due to the role of b_{ext_AN} and b_{ext_POM}, whereas many rural areas across the United States experienced maximum b_{ext_aer} during summer months, due to the role of b_{ext_POM} and b_{ext_AS}. The contributions of b_{ext_CM} were important in both urban and rural regions in the southwestern United States.

The highest annual mean b_{ext_AS} occurred at urban and rural sites in the eastern United States, where SO_2 emissions are greatest, and high RH in summer can facilitate hygroscopic growth. A strong spatial gradient occurred along the central United States, resulting in relatively low b_{ext_AS} at sites across the West, due to lower emissions. Contributions of b_{ext_AS} to b_{ext_aer} were also highest in the East, typically greater than 0.3, and highest at rural sites. With the exception of sites in Hawaii, the annual mean fractional contribution of b_{ext_AS} to b_{ext_aer} did not exceed 0.5 at any rural or urban site. Fractional contributions also decreased at sites toward the West. In the eastern United States, contributions reached an average maximum of 0.45 for IMPROVE regions and 0.37 for CSN regions, compared to the northwestern United States (0.35

and 0.26 for IMPROVE and CSN, respectively), and the southwestern United States (0.31 and 0.23 for IMPROVE and CSN, respectively).

Regional average monthly mean maximum b_{ext_AN} was higher in urban regions. For all CSN regions, the highest values occurred in regions in the southwestern United States. Rural estimates varied considerably depending on region, with average maximum values in the eastern United States, compared to the lowest maximum values in the southwestern United States. For nearly all regions, monthly mean maximum b_{ext_AN} was highest during winter months, reflecting favorable formation conditions. The fraction of b_{ext_aer} due to b_{ext_AN} was high at sites in the central United States, exceeding 0.3 across the region. Maximum contributions of b_{ext_AN} were similar for urban and rural regions in the eastern and northwestern Untied States (~0.4), but in the southwestern regions, higher contributions occurred in urban (0.36) relative to rural regions (0.23). These contributions were usually higher during winter months, except in some urban and rural regions in the southern part of California that had higher contributions year round.

Biomass smoke impacts at sites in the northwestern United States and Florida strongly influenced the b_{ext_POM} spatial pattern at rural sites, where the highest estimates of annual mean rural b_{ext_POM} occurred. Estimates were somewhat higher at sites in the southeastern United States, but still lower than at sites highly influenced by smoke. The annual mean b_{ext_POM} was higher in many urban areas, such as sites in the southeastern United States and the Central Valley of California, suggesting additional urban sources of POM. Average maximum contributions were higher in the northwestern United States and higher in IMPROVE regions (0.7 versus 0.5 in CSN regions). Although b_{ext_POM} contributions in urban and rural regions in the southwestern United States were higher than in the East, like in eastern regions they were similar in magnitude (~0.46–0.48).

The largest urban and rural differences were observed for monthly mean maximum b_{ext_EC}. Urban b_{ext_EC} was higher, with values four times higher in the eastern and southwestern United States and over two times higher in the northwestern United States. In most urban regions, b_{ext_EC} was higher during winter months, suggesting urban sources that led to higher b_{ext_EC} relative to summer biomass smoke influence. Contributions from b_{ext_EC} to b_{ext_aer} were also higher in urban regions for all areas. In the eastern United States, regional average urban maximum contributions of b_{ext_EC} were 0.16, compared to 0.09 in rural regions. This range was also observed in the northwestern United States (0.19 versus 0.10) and the southwestern United States (0.22 versus 0.11).

The average maximum b_{ext_FD} was similar at urban and rural regions across the United States. The highest monthly mean urban b_{ext_FD} occurred in regions in the eastern and southwestern United States, while rural regions experienced maximum b_{ext_FD} in the southwestern United States, a region known to experience frequent dust impacts. Similar spatial patterns in b_{ext_FD} and b_{ext_CM} also were observed at sites in the Central Valley of California, suggesting similar sources. However, unlike b_{ext_FD}, annual mean b_{ext_CM} was elevated at sites in the central United States, corresponding to areas of agricultural activity. Both b_{ext_FD} and b_{ext_CM} were elevated at sites in the southeastern United States and the Virgin Islands site, consistent with the influence of transport of dust from North Africa. The contributions of b_{ext_FD} and b_{ext_CM} to b_{ext_aer} were highest at sites in the southwestern United States, around ~0.05–0.15 and 0.2–0.3, respectively, for both urban and rural regions.

Visibility impacts of b_{ext_SS} were low, except in coastal regions. Average contributions of b_{ext_SS} to b_{ext_aer} in CSN regions were 0.01–0.02 and were somewhat higher in rural regions (0.05–0.07).

The spatial patterns in b_{ext_tot} and dv were similar and reflected the combined impacts from the species discussed above. Notably, the highest urban and rural b_{ext_tot} and dv occurred at sites in the central United States and the Central Valley of California. Both regions corresponded to sites with the highest b_{ext_AN}, suggesting the importance of agricultural activity on visibility in these regions. Lower b_{ext_tot} and dv occurred at sites along the Appalachian Mountains, the Northeast, and especially the Intermountain West. While the role of biomass smoke is important to b_{ext_tot}, with elevated levels at sites in the Northwest and Florida, the role of agriculture appeared to dominate. In both urban and rural regions, the role of b_{ext_AN} and b_{ext_POM} were very important, often driving the seasonality of the maximum b_{ext_aer} due to the seasonality of specific sources (e.g., biomass smoke during summer/fall) or during periods with favorable formation conditions (e.g., winter for b_{ext_AN}). However, b_{ext_AS} was within the top third contributing species in most regions, in part due to its hygroscopic nature, and was still an important contributor to b_{ext_aer}.

S.6 TRENDS IN IMPROVE SPECIATED AEROSOL MASS CONCENTRATIONS

One of the main purposes of the IMPROVE network is to document long-term trends for assessing progress towards the national visibility goals. Trend analyses were performed for long-term (1990–2019) and short-term (2000–2019) periods for eight parameters: annual, winter (DJF), spring (MAM), summer (JJA), and fall (SON) means, and 10^{th}, 50^{th}, and 90^{th} percentiles. Temporal trends were calculated for speciated mass concentrations, including sulfate ion, nitrate ion, OC, EC, FD, FM, PM_{10}, CM, as well as filter absorption (f_{abs}). Trends in SS or chloride ion are not presented because of negative biases in chloride concentrations from 2007 to 2011 (Zhang, 2019). Trends in CSN data were not evaluated because of the many changes that occurred starting in 2016 that resulted in some shifts to the data that require further evaluation before trends could be accurately interpreted (see Appendix 1.2). Full details for trend analyses for mass concentrations can be found in Chapter 6 and for b_{ext} in Chapter 7.

A Theil regression was performed with the concentration data as the dependent variable and the year as the independent variable (Theil, 1950). Completeness criteria are provided in Chapter 6. A trend was considered statistically significant at 5% ($p \leq 0.05$), meaning that there was a 95% chance that the slope was not due to random chance. "Trend" is defined as percent change per year (% yr^{-1}) and was computed by dividing the slope derived from the Theil regression by the median mass concentration or b_{ext} value over the period of the trend at a given site, multiplied by 100%. Reporting trends instead of slopes reflects the relative change in concentration or b_{ext} at a given site. However, trends can be quite large (>100%) when median concentrations or b_{ext} are very low (e.g., 10^{th} percentile).

Trend results were interpolated to provide isopleths to guide the eye Isaaks and Mohan Srivastava, 1989. Positive trends are denoted with an upward-pointing triangle and contoured with warm colors. Negative trends are shown with downward-pointing triangles and contoured with cold colors. Statistically significant trends ($p \leq 0.05$) are denoted with filled triangles. Scales were kept similar for all parameters so that trends can be compared. Only short-term

annual and seasonal mean trends for speciated mass are shown here; for additional results for both long-term and percentile trends for speciated mass and b_{ext}, see Chapters 6 and 7, respectively.

Short-term, regional mean trends were calculated for ten regions of the United States. Sites were grouped by their state into the following regions: Northeast, Southeast, Midsouth, Central, Southwest, Northwest, California, Alaska, Hawaii, Virgin Islands (see Table 6.0 and Figure 6.0 in Chapter 6) and the continental United States. The Virgin Islands region included one site. Although some names are the same, these regions are broader and do not necessarily correspond to the regions shown in Section S.4 and S.5 or Chapters 3 and 5. The regions were qualitatively determined only as a means for summarizing trends.

S.6.1 Sulfate Ion Trends

Annual mean short-term sulfate ion trends are shown in Figure S.6.1.1. Sulfate concentrations decreased for all of the short-term sites. The greatest decrease occurred for sites in the Appalachian area where SO_2 emissions have also dramatically decreased Hand et al., 2020. Sites east of -100° nearly all had concentrations decrease at rates greater than -4% yr^{-1}, and at sites in the Appalachia and Ohio River valley regions, trends were around -7% yr^{-1} to -10% yr^{-1}, corresponding to a 140–200% decrease over the past two decades. A strong spatial gradient in annual mean trends existed between the eastern and western United States, with weaker trends for sites in the West. Trends at sites in the western United States were about -2% yr^{-1} to -4% yr^{-1}. Insignificant trends occurred at sites in Hawaii, Alaska, and the Virgin Islands.

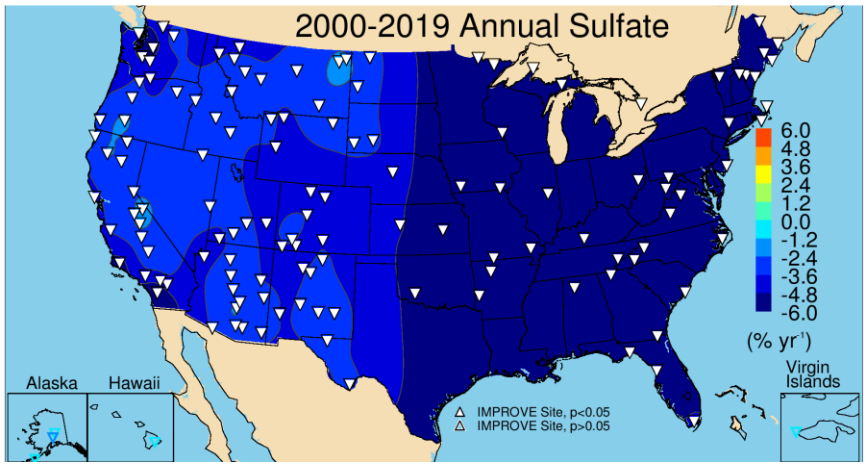

Figure S.6.1.1. Short-term (2000–2019) annual mean sulfate ion mass trends (% yr^{-1}). Filled triangles correspond to statistically significant trends ($p \leq 0.05$).

The spatial gradients and seasonal distribution in sulfate ion trends are also shown in the regional mean trends presented in Figure S.6.1.2, with regional mean trends ordered from west to east. The largest reductions in seasonal mean sulfate ion concentrations occurred for sites in the Northeast region (-10.56% yr^{-1} in summer), followed by the Southeast region (-9.46% yr^{-1} in fall). For the Northeast, Midsouth, and Central regions, the largest decrease in sulfate ion concentrations occurred during summer (in the Southeast decreases in fall were slightly larger), and the lowest decreases occurred during winter. This difference in the seasonal mean trends has led to a decrease in the seasonality of sulfate ion concentrations at eastern regions, as was

discussed in Section S.4.1 and Chapter 3. In regions in the western United States, the rate of decrease was lower, roughly half of the rate of decrease relative to eastern regions. The differences in seasonal mean trends were also smaller, suggesting that sulfate ion concentrations decreased by similar rates across seasons. The exception to this is the Southwest region, where the largest decreases occurred during both winter and fall. Overall, across the United States, sulfate ion concentrations have decreased at a higher rate during summer and fall. Seasonal mean trends at sites in Alaska, Hawaii, and the Virgin Islands were all relatively flat and insignificant.

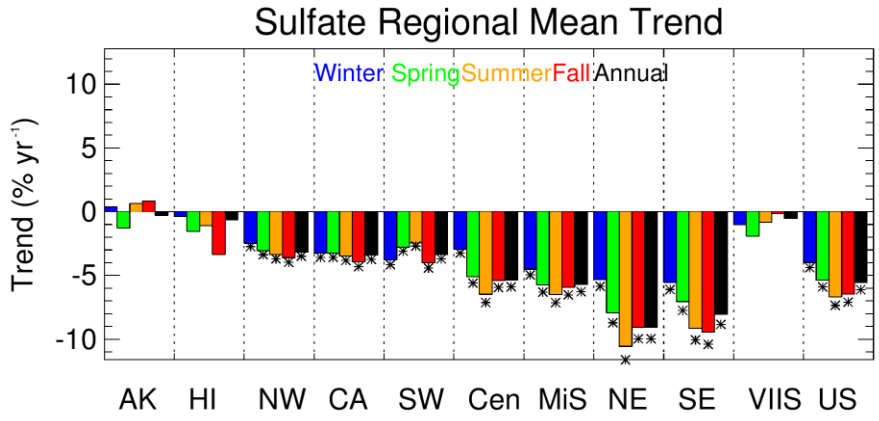

Figure S.6.1.2. Short-term (2000–2019) regional seasonal mean sulfate ion trends (% yr^{-1}) for major U.S. regions for winter, spring, summer, fall, and annual means. Regions are arranged from western to eastern United States (AK = Alaska, HI = Hawaii, NW = Northwest, CA = California, SW = Southwest, Cen = Central, MiS = Midsouth, NE = Northeast, SE = Southeast, VIIS = Virgin Islands, and US = all sites). Statistically significant trends ($p \leq 0.05$) are denoted with "*".

S.6.2 Nitrate Ion Trends

Short-term annual mean nitrate ion trends are shown in Figure S.6.2.1. The largest reductions in the annual mean nitrate ion concentrations occurred at sites in southern California (~-9% yr^{-1}). Strong reductions in nitrate ion concentrations in California are associated with reduced nitrogen dioxide emissions from vehicles (Krotkov et al., 2016; Hand et al., 2020). The strong east-west gradient observed for sulfate trends did not occur for nitrate trends. Insignificant trends occurred at sites in the northern Great Plains (-1% yr^{-1} to -2% yr^{-1}), likely due to the influence of oil and gas development in the region (Prenni et al., 2016; Evanoski-Cole et al., 2017; Gebhart et al., 2018).

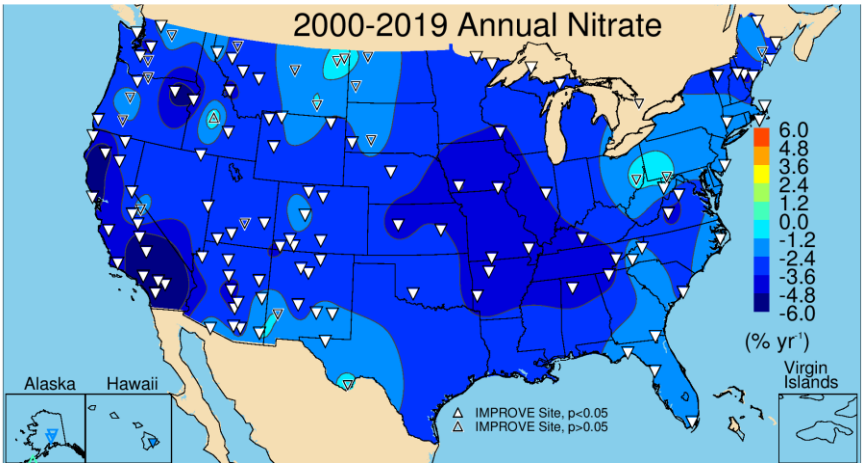

Figure S.6.2.1. Short-term (2000–2019) annual mean nitrate ion mass trends (% yr^{-1}). Filled triangles correspond to statistically significant trends ($p \leq 0.05$).

Comparisons of short-term regional, seasonal mean nitrate ion concentration trends are shown in Figure S.6.2.2. As seen in Figure S.6.2.1, the strongest reductions occurred in the California region, especially in fall (-7.46% yr^{-1}, $p < 0.001$) and spring (-7.00% yr^{-1}, $p < 0.001$). In other regions, there were differences in seasonal mean trends. For example, the regions of the Northwest, Southwest, and Southeast followed a similar pattern, with winter trends having the largest reductions, compared to the lowest reductions in summer, and spring and fall were in-between and comparable. This pattern is different from what occurred in the Midsouth region, with the strongest trends in spring, and the Central region, where the fall trends were the strongest and summer trends were lowest and insignificant. In contrast, very little range in seasonal trends occurred in the Northeast region (and winter had the lowest reductions). This range in seasonal mean trends indicates potentially different sources and atmospheric processes affecting nitrate concentrations in these regions.

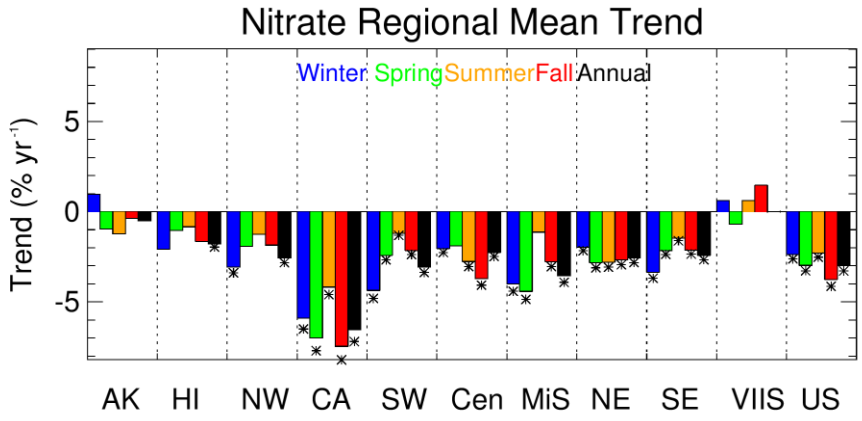

Figure S.6.2.2. Short-term (2000–2019) regional seasonal mean nitrate ion trends (% yr^{-1}) for major U.S. regions for winter, spring, summer, fall, and annual means. Regions are arranged from western to eastern United States (AK = Alaska, HI = Hawaii, NW = Northwest, CA = California, SW = Southwest, Cen = Central, MiS = Midsouth, NE = Northeast, SE = Southeast, VIIS = Virgin Islands, and US = all sites). Statistically significant trends ($p \leq 0.05$) are denoted with "*".

S.6.3 Organic Carbon Trends

Trends in OC and EC may be affected by changes in analytical methods. A recent review of carbonaceous measurements in the IMPROVE program identified shifts in analytical methods and their impacts on the fraction of EC to total carbon (OC + EC), i.e., EC/TC (Schichtel et al., 2021). Other shifts in EC/TC have also occurred over the history of the program due to new analyzers, new calibrations, and undetermined reasons. These effects have motivated discussions regarding future carbonaceous aerosol measurements within the program (Schichtel et al., 2021).

Annual mean OC trends are shown in Figure S.6.3.1. Relatively strong reductions in annual mean OC occurred at sites in the eastern and northeastern United States. In the western United States, strong reductions also occurred at sites in southern California and parts of Arizona and New Mexico. Insignificant short-term trends occurred at sites in Montana, Idaho, and Washington, where biomass smoke has influenced trends in particulate matter and OC (McClure and Jaffe, 2018). Although insignificant, many of the trends at sites in the northwestern United States were positive.

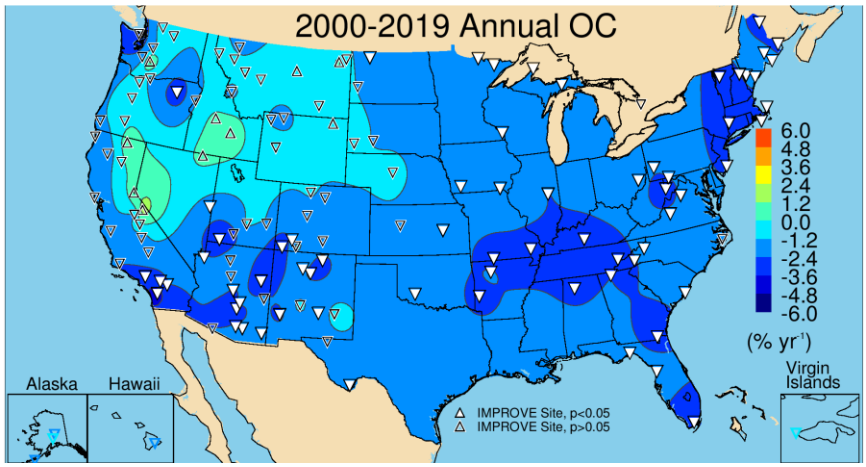

Figure S.6.3.1. Short-term (2000–2019) annual mean organic carbon (OC) mass trends (% yr^{-1}). Filled triangles correspond to statistically significant trends ($p \leq 0.05$).

Regional seasonal mean OC trends are shown in Figure S.6.3.2. Statistically significant trends occurred during all seasons in the Southeast, Northeast, and the Midsouth regions, about -3% yr^{-1}. The strongest reductions in most these regions occurred for winter and spring. Trends in the Central region were lower (~-2% yr^{-1}) than regions in the East and statistically significant in all seasons except summer. Seasonal mean trends at western regions were more variable than in the East. All of the winter and spring trends were statistically significant, and OC declined more strongly in these months (-3% yr^{-1} to -4% yr^{-1}). Summer and fall trends were insignificant and summer trends were flat in the Northwest and California regions. Trends during these seasons have been influenced by biomass burning emissions.

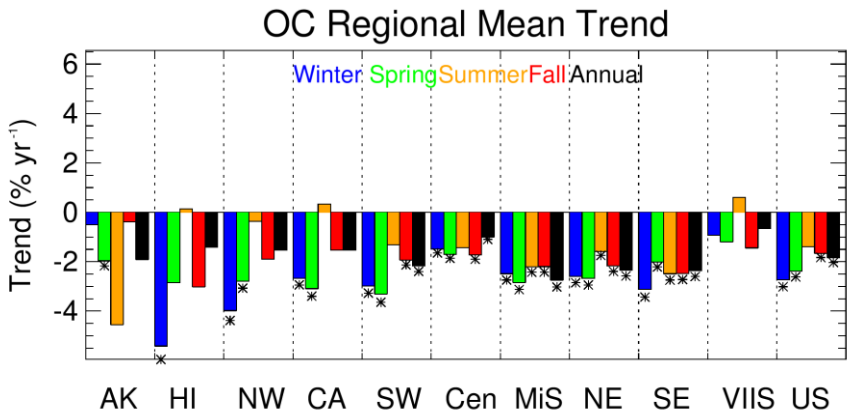

Figure S.6.3.2. Short-term (2000–2019) regional seasonal mean organic carbon (OC) trends (% yr^{-1}) for major U.S. regions for winter, spring, summer, fall, and annual means. Regions are arranged from western to eastern United States (AK = Alaska, HI = Hawaii, NW = Northwest, CA = California, SW = Southwest, Cen = Central, MiS = Midsouth, NE = Northeast, SE = Southeast, VIIS = Virgin Islands, and US = all sites). Statistically significant trends ($p \leq 0.05$) are denoted with "*".

S.6.4 Elemental Carbon Trends

EC trends are affected by hardware and analytic changes, similar to issues that affect OC trends. In addition, Malm et al. (2020) suggested EC may be inadvertently and incorrectly assigned to the OC fraction during the TOA, resulting in an underestimate of true EC concentrations. As discussed by Schichtel et al. (2021), EC concentrations have decreased at rural sites to the point that many sites have concentrations that are below the lower quantifiable limits (LQL, defined as 3 × minimum detection limit, MDL). From 2017 to 2019, about 30% of all EC concentrations were below the LQL. More sites in the West were below LQL than in the East. These low concentrations make tracking trends difficult, especially for the 10^{th} percentile concentrations.

Most of the short-term annual mean EC trends shown in Figure S.6.4.1 were negative and statistically significant. Sites with the strongest reductions (-5 to -6% yr^{-1}) were located in southern California, the northwestern United States, and regions of the northeastern United States. Most of the statistically insignificant trends occurred in the West at sites influenced by biomass smoke and in northern Montana and North Dakota, where oil and gas development has been demonstrated to impact EC concentrations (Gebhart et al., 2018).

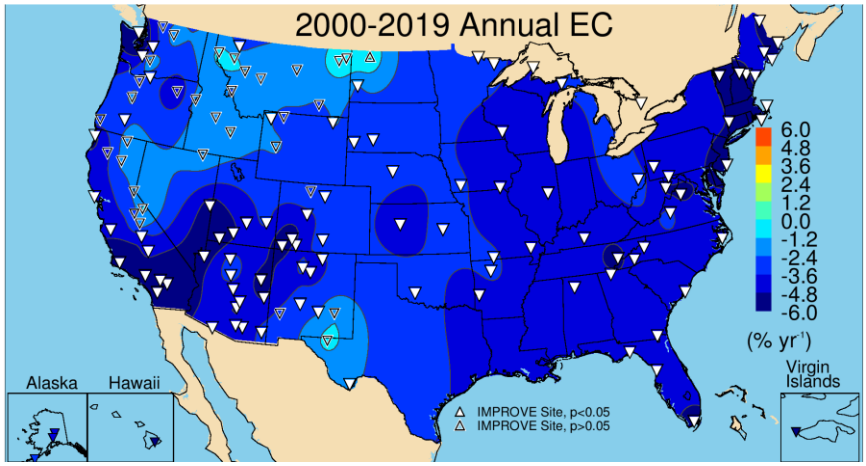

Figure S.6.4.1. Short-term (2000–2019) annual mean elemental carbon (EC) mass trends (% yr^{-1}). Filled triangles correspond to statistically significant trends ($p \leq 0.05$).

A summary of short-term regional, seasonal mean trends is shown in Figure S.6.4.2. Negative trends occurred for all regions and seasons. In regions in the eastern United States, the largest negative trends occurred during summer. Trends in the Southeast region were somewhat larger than other eastern regions, especially in winter and summer. The lowest negative trends occurred in the Central region, similar to OC trends. In the West, the strongest reductions in EC occurred mainly in winter and spring (e.g., California). Summer trends were weakest, and in the Northwest region were insignificant, likely reflecting the role of biomass smoke on EC concentrations. The difference in seasonal and regional trends implies different sources influencing EC depending on region.

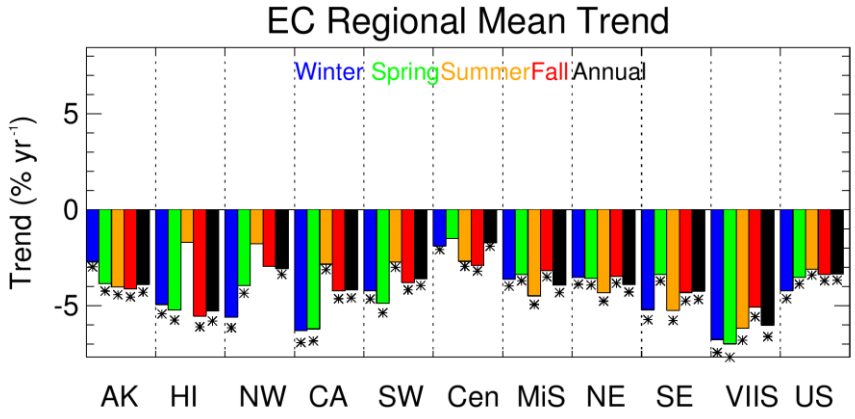

Figure S.6.4.2. Short-term (2000–2019) regional seasonal mean elemental carbon (EC) trends (% yr^{-1}) for major U.S. regions for winter, spring, summer, fall, and annual means. Regions are arranged from western to eastern United States (AK = Alaska, HI = Hawaii, NW = Northwest, CA = California, SW = Southwest, Cen = Central, MiS = Midsouth, NE = Northeast, SE = Southeast, VIIS = Virgin Islands, and US = all sites). Statistically significant trends ($p \leq 0.05$) are denoted with "*".

S.6.5 Fine Dust Trends

The analytical methods used to determine elemental species used to calculate FD (see Chapter 2) have evolved over time and included PIXE (proton induced X-ray emission) and XRF

(X-ray fluorescence) techniques. The transitions from PIXE to XFR methods, the change in XRF anodes from molybdenum to copper, as well as different calibration procedures affect the data by changing MDLs (Hyslop et al., 2015). In 2011, the analysis method switched to the PANalytical XRF system that resolved issues related to undetected Al with concentrations above the MDL (White, 2006). Before 2011, XRF data below the MDL were replaced by 0.5 × MDL. Changes in analytical methods may not equally affect data for each FD species; therefore, the integrated FD concentration may be less susceptible to possible variability introduced by the analytical methods, although this has not been specifically demonstrated.

Annual mean trends in FD for 2000–2019 at sites across the eastern United States were significantly negative, especially at sites in the northeastern United States, and across the Intermountain West and northwestern United States (see Figure S.6.5.1). Many insignificant and positive trends occurred at sites near the Central Valley of California, Oklahoma, Texas, Oregon, and North Dakota. Many of the sites in the southwestern United States had statistically insignificant trends.

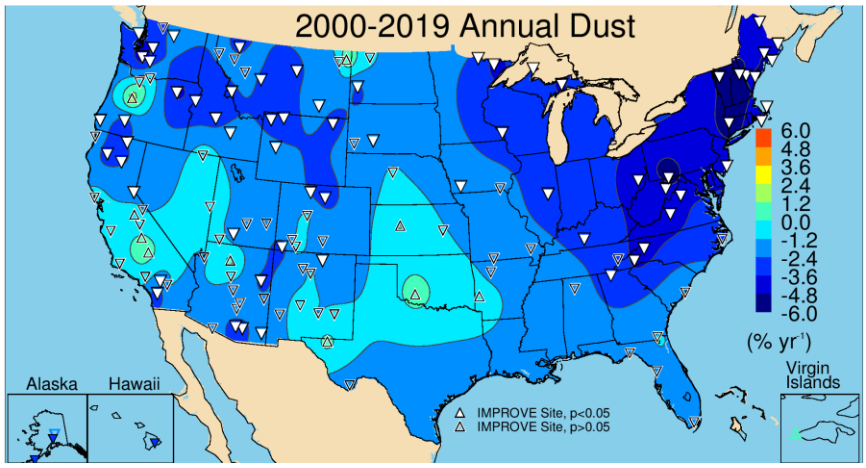

Figure S.6.5.1. Short-term (2000–2019) annual mean fine dust (FD) mass trends (% yr^{-1}). Filled triangles correspond to statistically significant trends ($p \leq 0.05$).

Compared to other species, trends in FD showed greater seasonal and spatial variability (Figure S.6.5.2). Trends were mostly insignificant and generally not strongly negative as is the case for other species. The Northeast region was the only region with statistically significant trends during all seasons. The Southeast region had statistically significant reductions in FD during all seasons except summer. Similarly, the Midsouth region had insignificant but positive trends during summer; this is the season with impacts from North African dust transport. In the Central region, only winter and spring corresponded to statistically significant negative trends. Across the West, regions were associated with insignificant though negative trends. The California region had insignificant but positive trends during summer, and the summer trends in the Northwest region were flat. FD has not experienced the levels of reduction that have occurred for other species.

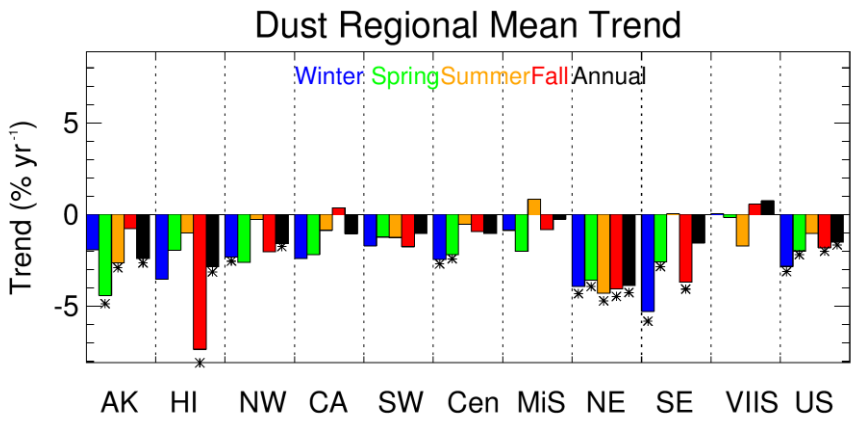

Figure S.6.5.2. Short-term (2000–2019) regional seasonal mean fine dust mass trends (% yr^{-1}) for major U.S. regions for winter, spring, summer, fall, and annual means. Regions are arranged from western to eastern United States (AK = Alaska, HI = Hawaii, NW = Northwest, CA = California, SW = Southwest, Cen = Central, MiS = Midsouth, NE = Northeast, SE = Southeast, VIIS = Virgin Islands, and US = all sites). Statistically significant trends ($p \leq 0.05$) are denoted with "*".

S.6.6 Gravimetric $PM_{2.5}$ Fine Mass Trends

Trends in FM may be driven by trends in a particular species, depending on the degree of its contribution; however, inferring FM trends based on the trends of other species is complicated because of the spatial and seasonal variability of a specific species relative to another. The statistical significance level of trends at a given site differs for each species and for FM trends, complicating comparisons of trends from different species at a specific location. In addition, sampling or analytical artifacts, such as particle bound water, may influence FM trends (see Chapter 1, Section 1.3.1.2). For example, beginning in 2011, higher laboratory relative humidity during weighing resulted in an increase in particle bound water associated with FM data (White, 2016). This issue was resolved in 2019, but it may influence trends in FM (Hand et al., 2019b).

Short-term trends in annual mean FM are shown in Figure S.6.6.1. The strongest trends in FM at sites in the eastern United States was likely associated with sulfate reductions. Of the 134 valid short-term sites, only 78 were associated with statistically significant trends, and nearly all of the insignificant trends occurred at sites in the western United States, especially at sites in the Intermountain West, northwestern United States, and northern California, where OC trends were also insignificant. Sites in southern California had strong negative trends, likely associated with nitrate ion reductions.

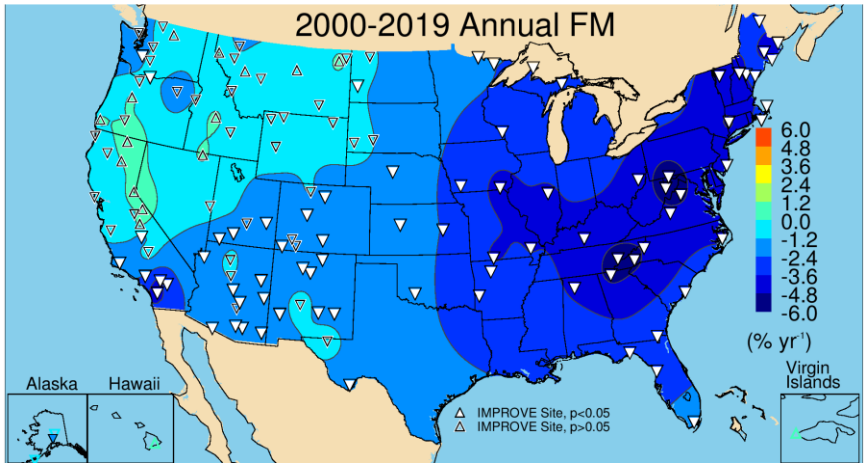

Figure S.6.6.1. Short-term (2000–2019) annual mean $PM_{2.5}$ gravimetric fine mass (FM) trends (% yr^{-1}). Filled triangles correspond to statistically significant trends ($p \leq 0.05$).

The short-term regional, seasonal mean trends in the eastern United States (Figure S.6.6.2) were similar to regional seasonal mean sulfate trends (compare Figure S.6.6.1 to Figure S.6.1.1). The strongest reductions in FM occurred in the Northeast and Southeast regions (-4% yr^{-1} to -5% yr^{-1}). Trends were weaker moving west, and in regions such as the Northwest and California, FM trends were similar to OC trends. Summer and fall trends in these regions were insignificant and positive, indicating the role of biomass smoke in FM trends. In the Southwest region, all of the seasons except summer had statistically significant reductions in FM. Only summer had an insignificant (negative) trend, similar to both OC and FD trends.

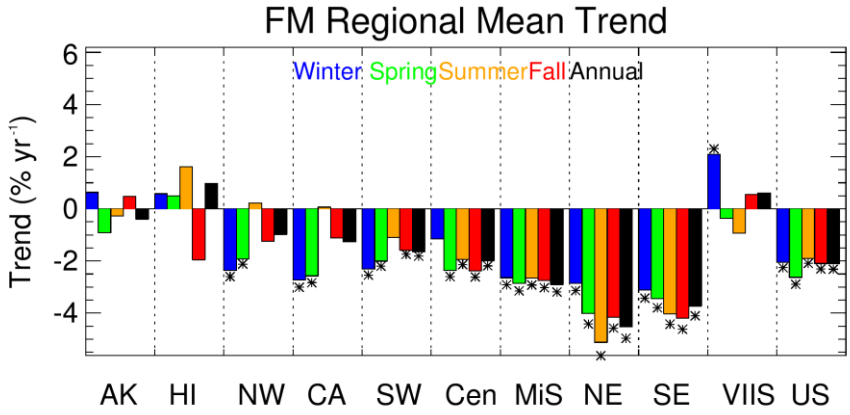

Figure S.6.6.2. Short-term (2000–2019) regional seasonal mean gravimetric $PM_{2.5}$ fine mass (FM) trends (% yr^{-1}) for major U.S. regions for winter, spring, summer, fall, and annual means. Regions are arranged from western to eastern United States (AK = Alaska, HI = Hawaii, NW = Northwest, CA = California, SW = Southwest, Cen = Central, MiS = Midsouth, NE = Northeast, SE = Southeast, VIIS = Virgin Islands, and US = all sites). Statistically significant trends ($p \leq 0.05$) are denoted with "*".

S.6.7 Coarse Mass Trends

Short-term annual mean CM trends are shown in Figure S.6.7.1. Unlike trends in FM, only 23 of 131 valid sites had statistically significant trends, suggesting that at most sites, trends were variable. CM declined significantly at some sites, for example, in Colorado, Wyoming, and

Montana, and in Arkansas. Positive trends (mostly insignificant) occurred at 61 sites, with six being statistically significant. The spatial pattern in short-term CM trends was different from FD trends (Figure S.6.6.1), suggesting that different composition or size distribution of coarse-mode aerosols influenced CM trends.

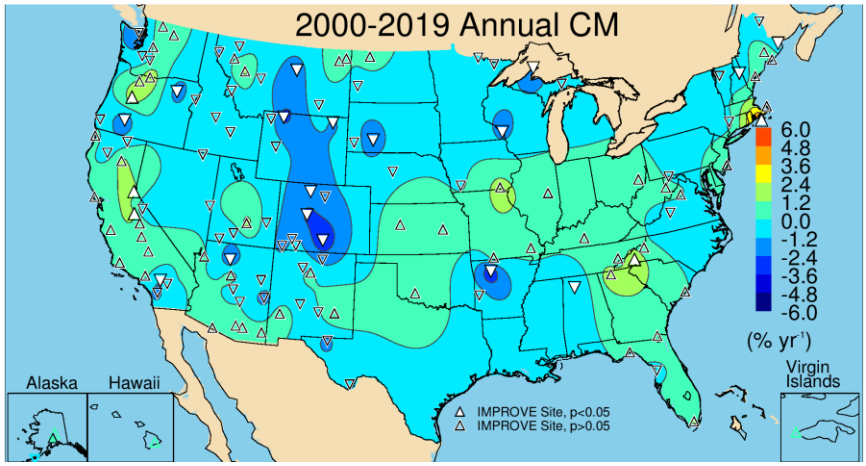

Figure S.6.7.1 Short-term annual mean (2000–2019) coarse mass (CM) trends (% yr^{-1}). Filled triangles correspond to statistically significant trends ($p \leq 0.05$).

Regional seasonal mean trends are shown in Figure S.6.7.2. As suggested in Figure S.6.7.1, nearly all of the regions were associated with insignificant and weak trends, especially relative to other species already discussed. The Northeast region had significant positive trends in summer, as did the Alaska and Hawaii regions. All of the seasonal mean trends in the Central region were positive but insignificant. The Midsouth and Southwest regions had weak but negative and insignificant trends, while the California region had weak, positive insignificant trends in summer and fall but negative, insignificant trends in winter and spring, The Northwest region had statistically significant trends in winter but weak and insignificant trends during other seasons.

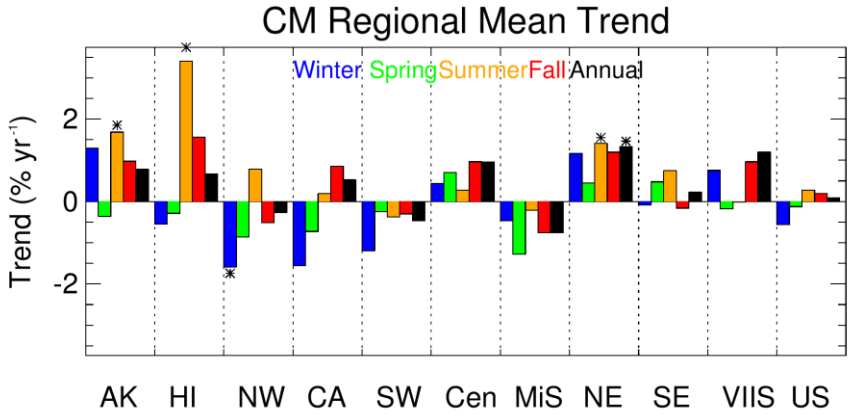

Figure S.6.7.2. Short-term (2000–2019) regional seasonal mean coarse mass (CM) trends (% yr^{-1}) for major U.S. regions for winter, spring, summer, fall, and annual means. Regions are arranged from western to eastern United States (AK = Alaska, HI = Hawaii, NW = Northwest, CA = California, SW = Southwest, Cen = Central, MiS = Midsouth, NE = Northeast, SE = Southeast, VIIS = Virgin Islands, and US = all sites). Statistically significant trends ($p \leq 0.05$) are denoted with "*".

S.6.8 Discussion

Timelines of regional, annual mean mass concentrations for $PM_{2.5}$ sulfate ion, nitrate ion, OC, EC, and FD corresponding to previous trend results are shown in Figure S.6.8 (a-j). Similar timelines for CM concentrations can be found in Chapter 6. These mass concentrations do not include mass correction factors for sulfate, nitrate, or OC (e.g., concentrations are for sulfate ion, not ammonium sulfate); therefore, the sum of individual bars should not be interpreted as RCFM, such as is shown in Chapter 3. However, the basic patterns are similar and reflect both RCFM and FM. It is clear from these timelines and the previous trend discussions that strong reductions in FM have occurred at nearly all remote regions across the United States. These reductions were greatest in the East and driven by strong negative trends in sulfate ion concentrations. Sulfate concentrations have decreased in response to dramatic reductions in SO_2 emissions due to regulatory activity (Hand et al., 2020). In addition, reductions in nitrate ion and OC concentrations (especially in the East) have contributed to reduced FM. Negative trends in nitrate concentrations at sites in southern California occurred where nitrogen dioxide emissions, especially mobile emissions, have declined due to regulatory activity.

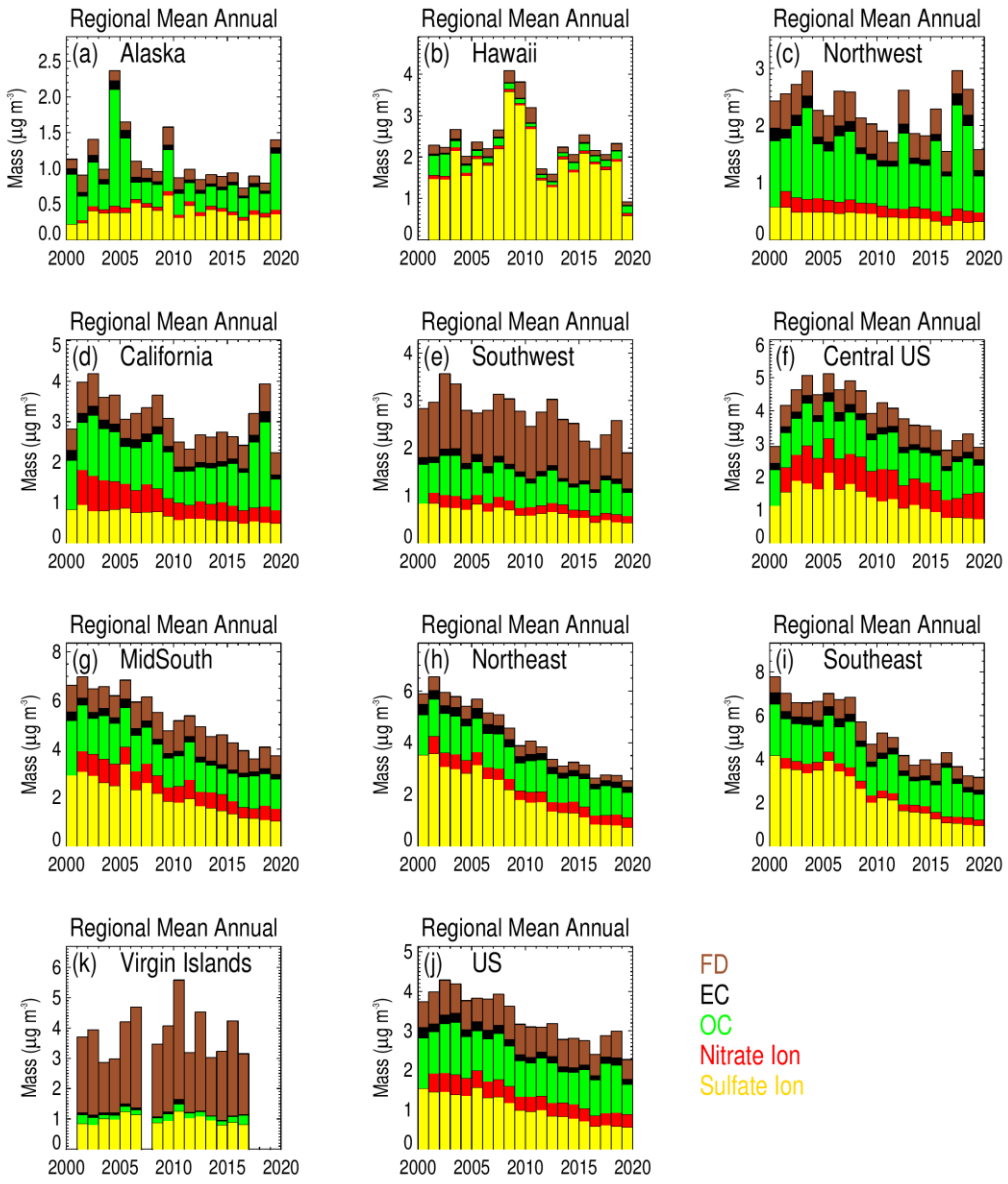

Figure S.6.8. Short-term (2001–2019) timelines of IMPROVE regional, annual mean mass concentrations (µg m^{-3}) for sulfate ion, nitrate ion, organic carbon (OC), elemental carbon (EC), and fine dust (FD).

At sites in the western United States, especially the Northwest, FM has declined at a weaker rate relative to sites in the East. Comparisons of OC and EC trends suggest that FM is influenced by biomass burning impacts that have led to an increase in OC, or at the very least flat and insignificant trends. OC is a major contributor to FM, especially at western sites, and has influenced FM trends in the region (McClure and Jaffe, 2018).

FM concentrations at sites in the Southwest have decreased (many insignificantly), although to a lower extent relative to sites in the East. The FM budget at these sites includes a significant fraction of FD, and trends in FD were insignificant. OC trends were also insignificant at many southwestern sites, suggesting that the role of FD and OC may have influenced FM trends in the region.

CM trends were notably different from trends in $PM_{2.5}$ speciated mass trends in that only a few sites across the United States had statistically significant negative CM trends. Several sites had statistically significant positive trends. Many of these sites did not have positive trends in FD, suggesting that CM may be associated with larger particles or species other than mineral dust.

Regulatory activity has been very successful at reducing pollutant emissions that lead to secondary aerosols, such as sulfate, nitrate, and OC, as well as reductions in primary aerosols such as EC, and some OC, depending on its sources. Reductions in these species have driven negative trends in FM and PM_{10} at sites across the United States. However, the role of natural aerosols, such as those derived from biomass smoke and dust storms have not declined and for some sites and seasons have increased. The impact of these positive trends have and likely will continue to impede progress in reducing FM and PM_{10} concentrations.

REFERENCES

Chow, J. C., Watson, J. G., Pritchett, L. C., Pierson, W. R., Frazier, C. A., and Purcell, R. G. (1993), The DRI thermal/optical reflectance carbon analysis system: description, evaluation and applications in US air quality studies, *Atmospheric Environment. Part A. General Topics*, *27*(8), 1185-1201, doi:https://doi.org/10.1016/0960-1686(93)90245-T.

Debell, L. J., Gebhart, K., Hand, J. L., Malm, W. C., Pitchford, M. L., Schichtel, B. S., and White, W. H. (2006), IMPROVE (Interagency Monitoring of Protected Visual Environments): Spatial and seasonal patterns and temporal variability of haze and its constituents in the United States: Report IV, *Colorado State University, Fort Collins CO*, *4*.

Evanoski-Cole, A., Gebhart, K., Sive, B., Zhou, Y., Capps, S., Day, D., Prenni, A., Schurman, M., Sullivan, A., and Li, Y. (2017), Composition and sources of winter haze in the Bakken oil and gas extraction region, *Atmospheric Environment*, *156*, 77-87, doi:http://dx.doi.org/10.1016/j.atmosenv.2017.02.019.

Gebhart, K. A., Day, D. E., Prenni, A. J., Schichtel, B. A., Hand, J. L., and Evanoski-Cole, A. R. (2018), Visibility impacts at Class I areas near the Bakken oil and gas development, *Journal of the Air & Waste Management Association*, *68*(5), 477-493, doi:10.1080/10962247.2018.1429334.

Gorham, K. A., Raffuse, S. M., Hyslop, N. P., and White, W. H. (2021), Comparison of recent speciated PM2. 5 data from collocated CSN and IMPROVE measurements, *Atmospheric Environment*, *244*, 117977, doi:https://doi.org/10.1016/j.atmosenv.2020.117977.

Hand, J. L., Copeland, S., Day, D., Dillner, A., Indresand, H., Malm, W., McDade, C., Moore, C., Pitchford, M., and Schichtel, B. (2011), IMPROVE (Interagency Monitoring of Protected Visual Environments): Spatial and seasonal patterns and temporal variability of haze and its constituents in the United States, *CIRA Report*, *5*.

Hand, J. L., Gill, T., and Schichtel, B. (2017), Spatial and seasonal variability in fine mineral dust and coarse aerosol mass at remote sites across the United States, *Journal of Geophysical Research: Atmospheres*, *122*(5), 3080-3097, doi:doi:10.1002/2016JD026290.

Hand, J. L., Gill, T. E., and Schichtel, B. A. (2019a), Urban and rural coarse aerosol mass across the United States: Spatial and seasonal variability and long-term trends, *Atmospheric Environment*, *218*, 117025, doi:doi.org/10.1016/j.atmosenv.2019.117025.

Hand, J. L., Prenni, A. J., Schichtel, B. A., Malm, W. C., and Chow, J. C. (2019b), Trends in remote PM2.5 residual mass across the United States: Implications for aerosol mass reconstruction in the IMPROVE network, *Atmospheric Environment*, *203*, 141-152, doi:doi:10.1016/j.atmosenv.2019.01.049.

Hand, J. L., Prenni, A. J., Copeland, S., Schichtel, B. A., and Malm, W. C. (2020), Thirty years of the Clean Air Act Amendments: Impacts on haze in remote regions of the United States

(1990–2018), *Atmospheric Environment*, *243*, 117865, doi:https://doi.org/10.1016/j.atmosenv.2020.117865.

Hyslop, N. P., Trzepla, K., and White, W. H. (2015), Assessing the suitability of historical PM2. 5 element measurements for trend analysis, *Environmental Science & Technology*, *49*(15), 9247-9255, doi:DOI: 10.1021/acs.est.5b01572.

Isaaks, E. H., and Mohan Srivastava, R. (1989), *An Introduction to Applied Geostatistics*, Oxford University Press, New York, 978-0195050134.

Krotkov, N. A., McLinden, C. A., Li, C., Lamsal, L. N., Celarier, E. A., Marchenko, S. V., Swartz, W. H., Bucsela, E. J., Joiner, J., Duncan, B. N., Boersma, K. F., Veefkind, J. P., Levelt, P. F., Fioletov, V. E., Dickerson, R. R., He, H., Lu, Z., and Streets, D. G. (2016), Aura OMI observations of regional SO2 and NO2 pollution changes from 2005 to 2015, *Atmos. Chem. Phys.*, *16*(7), 4605-4629, doi:10.5194/acp-16-4605-2016.

Lambert, A., Hallar, A. G., Garcia, M., Strong, C., Andrews, E., and Hand, J. L. (2020), Dust impacts of rapid agricultural expansion on the Great Plains, *Geophysical Research Letters*, *47*(20), e2020GL090347, doi:https://doi.org/10.1029/2020GL090347.

Malm, W., Sisler, J. F., Pitchford, M., Scruggs, M., Ames, R. B., Copeland, S., Gebhart, K., and Day, D. (2000), IMPROVE (Interagency Monitoring of Protected Visual Environments): Spatial and seasonal patterns and temporal variability of haze and its constituents in the United States: Report III, *CIRA Report*, *3*.

Malm, W., Schichtel, B., Hand, J., and Prenni, A. (2020), Implications of organic mass to carbon ratios increasing over time in the rural United States, *Journal of Geophysical Research: Atmospheres*, *125*(5), e2019JD031480.

McClure, C. D., and Jaffe, D. A. (2018), US particulate matter air quality improves except in wildfire-prone areas, *Proceedings of the National Academy of Sciences*, *115*(31), 7901-7906, doi:doi:10.1073/pnas.1804353115.

Pitchford, M. L., and Malm, W. C. (1994), Development and applications of a standard visual index, *Atmospheric Environment*, *28*(5), 1049-1054, doi:https://doi.org/10.1016/1352-2310(94)90264-X.

Prenni, A., Day, D., Evanoski-Cole, A., Sive, B., Hecobian, A., Zhou, Y., Gebhart, K., Hand, J., Sullivan, A., and Li, Y. (2016), Oil and gas impacts on air quality in federal lands in the Bakken region: an overview of the Bakken Air Quality Study and first results, *Atmospheric Chemistry and Physics*, *16*(3), 1401-1416, doi:doi:10.5194/acp-16-1401-2016.

Schichtel, B. A., Malm, W. C., Beaver, M., Copeland, S., Hand, J. L., Prenni, A. J., Rice, J., and Vimont, J. (2021), The Future of Carbonaceous Aerosol Measurement in the IMPROVE Monitoring Program, http://vista.cira.colostate.edu/improve/wp-content/uploads/2021/10/041_CarbonReport_Final.pdf.

Sisler, J. F., Huffman, D., Latimer, D. A., Malm, W. C., and Pitchford, M. (1993), IMPROVE (Interagency Monitoring of Protected Visual Environments): Spatial and Temporal Patterns and the Chemical Composition of the Haze in the United States: An Analysis of Data from the IMPROVE Network, 1988-1991: Report I *Colorado State University, Fort Collins CO, 1*.

Sisler, J. F., Malm, W. C., Gebhart, K., and Pitchford, M. (1996), IMPROVE (Interagency Monitoring of Protected Visual Environments): Spatial and Seasonal Patterns and Long Term Variability of the Composition of the Haze in the United States: An Analysis of Data from the IMPROVE Network, 1996: Report II, *Colorado State University, Fort Collins CO, 2*.

Solomon, P. A., Crumpler, D., Flanagan, J. B., Jayanty, R. K. M., Rickman, E. E., and McDade, C. E. (2014), U.S. National PM2.5 Chemical speciation monitoring networks—CSN and IMPROVE: Description of networks, *Journal of the Air & Waste Management Association, 64*(12), 1410-1438, doi:doi:10.1080/10962247.2014.956904.

Theil, H. (1950), A rank-invariant method of linear and polynomial regression analysis., *Proc. Kon. Ned. Akad. v Wetensch., A*(53), 386-392, doi:https://doi.org/10.1007/978094-011-2546-8_20.

White, W. H. (2006), Elemental concentrations above the MDL can go undetected, *IMPROVE Data Advisory* (da0010), http://vista.cira.colostate.edu/improve/Data/QA_QC/Advisory/da0010/da0010_Almdl.pdf.

White, W. H. (2016), Increased variation of humidity in the weighing laboratory, *IMPROVE Data Advisory* (da0035), http://vista.cira.colostate.edu/improve/Data/QA_QC/Advisory/da0035/da0035_IncreasedRH.pdf.

Zhang, X. (2019), Correction of chloride concentrations for filter blank levels, *IMPROVE Data Advisory* (da0039), http://vista.cira.colostate.edu/improve/Data/QA_QC/Advisory/da0039/da0039_ChlorideOverCorrection.pdf.